# ADVANCED SULFUR CONTROL CONCEPTS IN HOT-GAS DESULFURIZATION TECHNOLOGY: PHASE 2. EXPLORATORY STUDIES ON THE DIRECT PRODUCTION OF ELEMENTAL SULFUR DURING THE REGENERATION OF HIGH TEMPERATURE DESULFURIZATION SORBENTS

Topical Report

A. Lopez
W. Huang
J. White
Y. Zeng
F.R. Groves
D.P. Harrison



July 1997

Work Performed Under Contract No.: DE-AC21-94MC30012--13

for
Federal Energy Technology Center
Morgantown, West Virginia



by
Louisiana State University
Department of Chemical Engineering
Baton Rouge, Louisiana

## DISCLAIMER

## DISCLAIMER

Portions of this document may be illegible electronic image products. Images are produced from the best available original document.

## ACKNOWLEDGMENT

This research is sponsored by the U.S. Department of Energy, Federal Energy Technology Center under contract number DE-AC21-94MC30012. The authors are particularly grateful for the assistance and advice provided by Mr. Thomas Dorchak of FETC.

## EXECUTIVE SUMMARY

The topical report describes the results of Phase 2 research to determine the feasibility of the direct production of elemental sulfur during the regeneration of high temperature desulfurization sorbents. Results of Phase 1 research, which included a literature survey and thermodynamic analysis of elemental sulfur production, were presented in an earlier topical report dated October 1994.

The Federal Energy Technology Center - Morgantown of the U.S. Department of Energy has primary responsibility for the development of advanced power systems to enable the nation's vast coal reserves to be used in an economical and environmentally acceptable manner. Integrated gasification combined cycle (IGCC) technology has emerged as a major thrust in meeting this responsibility. IGCC power plants are attractive because of their low emissions and increased electrical generation efficiency.

Many of the contaminants present in coal emerge from the gasification process in the product gas. The contaminants, in the form of $H_2S$, $NH_3$, halogens, etc., must be removed prior to power generation. Using current technology, these contaminants can only be removed at low temperature. This requires that the coal gas be cooled, treated, and reheated prior to power generation. The purification process would be simplified and the overall thermodynamic efficiency increased if the contaminants could be removed at high temperature.

Much effort has gone into the development of high temperature metal oxide sorbents for removal of $H_2S$ from coal gas. The oxides of zinc, iron, manganese, and others have been studied. In order for high temperature desulfurization to be economical it is necessary that the sorbents be regenerated to permit multicycle operation. Current methods of sorbent regeneration involve oxidation of the metal sulfide to reform the metal oxide and free the sulfur as $SO_2$. There are a number of problems associated with this method of regeneration. The oxidation reaction is highly exothermic, which complicates the problem of regeneration reactor temperature control and may hasten sorbent deterioration through sintering. Limiting regenerator temperature excursions may be accomplished by diluting the oxygen in the regeneration feed gas. This approach reduces the $SO_2$ concentration in the regeneration product gas and complicates the ultimate $SO_2$ control problem. Finally, the sulfates of many of the candidate sorbents may be formed in the $SO_2$ - $O_2$ atmosphere. Spalling caused by the formation of the $ZnSO_4$ is one of the problems which has delayed the development of zinc-based sorbent processes.

An alternate regeneration process in which the sulfur is liberated in elemental form is desired. Elemental sulfur, which is the typical feed to sulfuric acid plants, may be easily separated, stored, and transported. Although research to convert $SO_2$ produced during sorbent regeneration to elemental sulfur is on-going, additional processing steps are required and the overall process will be more complex. Clearly, the direct production of elemental sulfur is preferred.

This study began with a literature search to identify possible concepts for elemental sulfur production during regeneration and to gather relevant thermodynamic, kinetic, and process data. Following the literature search, a thermodynamic analysis, based on free energy minimization, was carried out to evaluate candidate sorbents for possible use with the regeneration concepts. As a result of this effort, iron- and cerium-based sorbents were selected for the preliminary experimental study.

Neither of these materials possesses the high $H_2S$ removal capability associated with zinc-based sorbents. However, on the basis of the thermodynamic analysis, both are more likely to produce elemental sulfur during the regeneration phase.

The regeneration of FeS has been investigated using the so-called partial oxidation concept in which the regeneration feed gas contains large $H_2O/O_2$ ratios. Electrobalance reactor studies were performed initially to obtain comparative kinetics of the FeS-$O_2$ and FeS-$H_2O$ reactions. This was followed by a series of laboratory-scale fixed-bed reactor tests in which the distribution of sulfur species in the regeneration product gas was determined as a function of reaction time. Real time product gas analysis required the development of a new analytical method for simultaneous measurement of $SO_2$, $H_2S$, and elemental sulfur concentrations. Large portions of the sulfur originally present in FeS were liberated in elemental form. For example, instantaneous and cumulative elemental sulfur selectivities of greater than 80% and about 75% of theoretical, respectively, were measured. However, the large $H_2O/O_2$ ratio meant that the elemental sulfur concentration in the product gas was quite small. The large steam requirement was judged to render the process uneconomical.

The thermodynamic properties of $Ce_2O_2S$, the sulfided form of $CeO_2$, are unique in that regeneration to elemental sulfur is favored using each of the three regeneration concepts identified in the literature search. The most favorable concept is based on regeneration with $SO_2$ which is represented by the following reaction:

$$Ce_2O_2S(s) + SO_2(g) ==> 2CeO_2(s) + S_2(g)$$

This concept is basically free of side reactions, and the thermodynamics permit complete $Ce_2O_2S$ regeneration at 1000 K and 25 atm with less than 30% excess $SO_2$. Under these conditions, the regeneration product gas would contain about 85% elemental sulfur.

In contrast to zinc-based sorbents, problems associated with $CeO_2$ are associated primarily with the desulfurization step. $CeO_2$ is not thermodynamically capable of reducing $H_2S$ concentrations to the 20 ppmv target level. Therefore, a two-stage process in which $CeO_2$ would be used for bulk $H_2S$ removal, and a zinc-based sorbent would be used for $H_2S$ polishing has been proposed. Elemental sulfur is to be produced directly during $Ce_2O_2S$ regeneration while the relatively small quantity of ZnS is to be regenerated in the traditional manner using $O_2$ with the $SO_2$ recycled to the gasifier.

Preliminary tests involving the sulfidation of $CeO_2$ to $Ce_2O_2S$ and regeneration back to $CeO_2$ by reaction with $SO_2$ have been carried out in the fixed-bed reactor. Preparation of $Ce_2O_2S$ by sulfidation of $CeO_2$ is necessary since $Ce_2O_2S$ cannot be obtained commercially. Also, all cerium sorbent testing has been limited to the fixed-bed reactor; there is no change in solid mass involved in the conversion of $2CeO_2$ to $Ce_2O_2S$ so that no information can be gained from electrobalance reactor tests.

During sulfidation at 800°C, the $H_2S$ concentration during the prebreakthrough period has been reduced from 10,000 ppmv in the feed gas to 100 ppmv (or less) in the product gas. The

thermal conductivity detector used for $H_2S$ analysis is limited to approximately 100 ppmv. While there are indications that prebreakthrough $H_2S$ concentrations in the range of 20 to 40 ppmv have been achieved, the results at this concentration level are uncertain.

Quite favorable results have been obtained from tests involving the regeneration of $Ce_2O_2S$ with $SO_2$. At 600°C, the reaction is rapid and goes to completion. The $SO_2$ content of the regeneration feed gas has been as high at 12 mol %, and the elemental sulfur content of the product gas (measured as $S_2$) has approached 12% prior to $SO_2$ breakthrough. Ten complete sulfidation-regeneration cycles have been completed at the above conditions with no apparent deterioration in sorbent performance.

Favorable results from the experimental tests and on-going process analysis suggest that a desulfurization process using $CeO_2$-based sorbent is feasible. Additional experimental tests will be conducted during the remaining portion of the study to examine the effect of reaction conditions on both the sulfidation and regeneration performance.

Table of Contents

List of Figures

List of Tables

## INTRODUCTION

The integrated gasification combined cycle (IGCC) process, which combines coal gasification with electric power generation, creates the possibility of utilizing the nation's large coal reserves with greater efficiency and less environmental impact than the current pulverized coal-steam cycle. Efficiencies of approximately 50% are possible for an optimized IGCC process. The optimized process requires that a number of contaminants be removed from the high temperature coal gas prior to power generation. Control of particulate matter and a number of gaseous materials including sulfur compounds (primarily $H_2S$) is required. The sulfur compounds, which constitute the primary emphasis of this study, must be removed both to meet environmental standards and to prevent corrosion of the turbine blades.

Various liquid scrubbing processes, many utilizing an amine solvent, are available for $H_2S$ removal. However, such processes do not integrate well with the gasification and power generation sections of the IGCC process. Hot coal gases must be cooled to near ambient temperature, scrubbed, and then reheated prior to entering the power generation section. Energy losses, which reduce the efficiency of electricity generation, and gas-to-gas heat exchangers, which are necessarily large and expensive, are the inevitable result of liquid scrubbing processes for $H_2S$ removal.

High temperature desulfurization based on the noncatalytic reaction of $H_2S$ with an appropriate metal oxide sorbent can eliminate many of the problems associated with low temperature sulfur removal and allow the IGCC process to operate at higher efficiency. The general high temperature desulfurization reaction may be represented by

$$MeO(s) + H_2S(g) ==> MeS(s) + H_2O(g) \qquad (1)$$

Metal oxide sorbents having high sulfur capacity and the capability of reducing the $H_2S$ content of the coal gas to about 10 ppmv are available. However, economic considerations require that the sorbent be regenerable and able to withstand many sulfidation-regeneration cycles. For these reasons the sorbent must process good mechanical strength and be resistant to attrition and sintering at the temperatures of interest.

The regeneration reaction which has received the most attention in the past involves direct oxidation of both the metal and sulfur species. This reaction is represented generically by

$$MeS(s) + 1.5O_2(g) ==> MeO(s) + SO_2(g) \qquad (2)$$

Metal sulfate formation is often favored at lower temperatures, requiring the regeneration reaction to be carried out above the sulfate decomposition temperature. Reaction (2) is highly exothermic, leading to complex reactor temperature control problems and the possibility of sorbent deterioration due to sintering. In order to control the temperature, the regeneration feed gas may contain large concentrations of inert diluent. This results in small concentrations of $SO_2$ in the regeneration product gas and complicates the ultimate $SO_2$ control problem.

These regeneration problems would be eliminated, or at least greatly alleviated, if elemental sulfur instead of $SO_2$ could be produced during sorbent regeneration. Partial oxidation is less

exothermic so that reactor temperature control problems would be eased. Sulfate formation can be avoided, and, most importantly, elemental sulfur can be easily separated by condensation. Liquid or solid elemental sulfur product can be stored and transported relatively easily, and, as the standard feed to sulfuric acid plants, it has commercial value.

The initial phase of this project consisted of a literature review to identify concepts for the direct production of elemental sulfur. Three concepts were identified. The first, which we refer to as partial oxidation, involves reaction of the metal sulfide in an $H_2O/O_2$ atmosphere operated in an $O_2$-starved manner. While a number of simultaneous reactions occur, the net result can be represented by

$$MeS(s) + 0.5O_2(g) ==> MeO(s) + 0.5S_2(g) \quad (3)$$

The second concept involves the use of $SO_2$ as the oxidant according to the following stoichiometry

$$MeS(s) + 0.5SO_2(g) ==> MeO(s) + 0.75S_2(g) \quad (4)$$

The third concept represents a direct reversal of the sulfidation reaction by reacting the metal sulfide with steam

$$MeS(s) + H_2O(g) ==> MeO(s) + H_2S(g) \quad (5)$$

Although $H_2S$ rather than elemental sulfur is the reaction product, the concept was judged to be of interest if sufficiently high concentrations of $H_2S$ could be produced to permit the regeneration product to be fed to a Claus reactor for elemental sulfur recovery.

In the second phase of the project, the thermodynamics of the regeneration concepts were examined using a number of candidate sorbents. In general, we concluded that sorbents having the greatest affinity for $H_2S$ in the sulfidation phase were least amenable to the liberation of elemental sulfur during regeneration. There appeared to be little, if any, opportunity to produce elemental sulfur during the regeneration of ZnS. Iron-based sorbents are less efficient than zinc sorbents in removing $H_2S$ and, therefore, are somewhat more amenable to the liberation of elemental sulfur. In particular, the partial oxidation regeneration of FeS was judged to be of potential interest. This conclusion was based on previous literature results as well as from the thermodynamic analysis. Successful partial oxidation regeneration would operate under kinetic, rather than thermodynamic, control.

The thermodynamic properties of sorbents based on the oxides of tin and cerium were found to be unique in terms of $H_2S$ removal and the potential for elemental sulfur production during regeneration. While these oxides were thermodynamically less effective for $H_2S$ removal, elemental sulfur production was favored using each of the three regeneration concepts.

The iron and cerium sorbent systems were subsequently selected for the preliminary study, and results of these preliminary tests are described in this report. FeS regeneration has been studied using the partial oxidation concept in both electrobalance and fixed-bed reactors. Since sulfidation of iron oxide has been studied extensively, the experimental activity was limited to the regeneration

of FeS obtained from commercial sources. Cerium oxysulfide, $Ce_2O_2S$, is the product of the reaction between $CeO_2$ and $H_2S$. Since $Ce_2O_2S$ is not available commercially, both sulfidation and regeneration experiments were conducted. Regeneration tests used the reaction of $Ce_2O_2S$ with $SO_2$. Also, since there is no solid weight change in the conversion of $2CeO_2$ to $Ce_2O_2S$, the electrobalance reactor was not applicable. All experimental tests used a laboratory-scale fixed-bed reactor and the progress of the reaction was monitored by analyzing the composition of the product gas as a function of time.

## FeS PARTIAL OXIDATION

The electrobalance reactor was used to study the individual reactions of FeS with $O_2$ and with $H_2O$ from 600 to 800°C and from 1 to 15 atm. The gas composition ranged from 0.5 to 3.0% $O_2$ in $N_2$ and from 10 to 40% $H_2O$ in $N_2$. A limited number of tests were conducted using $O_2$-$H_2O$-$N_2$ mixtures with the $H_2O$ content fixed at 30% and the $O_2$ content varied from 0.05 to 0.5%. While a number of simultaneous reactions may occur, the experimental results can be interpreted on the basis of four primary reactions:

$$2FeS(s) + 3.5O_2(g) ==> Fe_2O_3(s) + 2SO_2(g) \quad (6)$$

$$3FeS(s) + 4H_2O(g) ==> Fe_3O_4(s) + 3H_2O(g) + H_2(g) \quad (7)$$

$$2H_2S(g) + SO_2(g) ==> 2H_2O(g) + 1.5S_2(g) \quad (8)$$

$$2Fe_3O_4(s) + 0.5O_2(g) ==> 3Fe_2O_3(s) \quad (9)$$

Only reaction (6) occurs in the $O_2$-$N_2$ atmosphere, while only reaction (7) occurs in $H_2O$-$N_2$. The Claus reaction (8) is believed to be primarily responsible for elemental sulfur formation, while $Fe_3O_4$(s) formed by reaction (7) is rapidly oxidized to $Fe_2O_3$(s) by reaction (9) when contacted by $O_2$. Elemental sulfur is represented in reaction (8) and elsewhere as $S_2$(g) for convenience. In reality, various quantifies of gaseous sulfur allotropes, $S_n$ with $8 \geq n \geq 1$, may be formed, depending on temperature and pressure.

In the electrobalance, the progress of the individual reactions (6) and (7) was followed by monitoring the change in solid mass which accompanied the conversion of FeS to either $Fe_2O_3$ or $Fe_3O_4$. The electrobalance reactor is of limited use when simultaneous gas-solid reactions occur and provides no information on gas phase reactions. Hence, the fixed-bed reactor with product gas analysis was used in most experiments when the feed gas contained both $O_2$ and $H_2O$. Fixed-bed tests were conducted at 4.4 atm over a temperature range of 550 to 700 °C. The feed gas contained 0 to 1.5% $O_2$, 0 to 52% $H_2O$ and balance $N_2$. The $H_2O/O_2$ ratio in the feed gas varied from 0 to 200. Development of an analytical method to determine the concentration of sulfur species -- $SO_2$, $H_2S$, and $S_2$ -- as a function of time required a major effort. The method is described in a subsequent section.

Approximately 3 mg of FeS from Johnson Matthey Co. were used in the electrobalance tests. The composition and selected properties of this material, as supplied by Johnson Matthey and as

measured at LSU, are presented in the top section of Table 1. The FeS used in the fixed-bed tests was from Strem Chemicals; composition and selected properties are found in the bottom section of Table 1. From 0.5 to 3.3 g of FeS were mixed with approximately three grams of $Al_2O_3$ in the fixed-bed reactor runs. The quantity of FeS depended on the flow rate and $O_2$ content of the regeneration feed gas and was adjusted so that the reaction could be completed in a reasonable time period. Selected properties of the $Al_2O_3$, which was added to minimize sintering, are also found in Table 1.

Table 1. FeS Composition and Properties

| | |
|---|---|
| Electrobalance Tests | |
| FeS Source | Johnson Matthey |
| Composition (Mass%) | |
| Fe | 61.78 |
| Al | <0.01 |
| Ca | <0.01 |
| Co | <0.01 |
| Cu | 0.02 |
| Mg | <0.01 |
| Mn | <0.01 |
| Ni | <0.01 |
| Particle Size Range | < 100 mesh |
| Specific Surface Area | 5.3 $m^2/g$ (Measured by LSU) |
| Fixed-Bed Tests | |
| FeS Source | Strem Chemicals |
| FeS Content | 99.2 $\pm$ 0.1% |
| Particle Size Range | 60 to 200 mesh |
| $Al_2O_3$ Source | Sigma Chemicals |
| Particle Size Range | 80 to 200 mesh |

**Electrobalance Studies**

**Equipment**: A schematic diagram of the high pressure electrobalance reactor system is shown in Figure 1. The electrobalance housing and reactor hangdown tube were constructed of 316 stainless steel capable of operating at 1500 psi at 600°C. The inner surface of the hangdown tube was Alonized to minimize interaction between $H_2S$ and metal. The FeS was held in a platium pan and suspended from the electrobalance with a nichrome wire.

Ultra high purity (UHP) $N_2$ was fed through the electrobalance housing to prevent back diffusion of reactive gases into the balance chamber. Additional UHP $N_2$, air, and/or steam were fed through an opening in the side of the hangdown tube. Combined gases flowed downward over the sorbent. Gases were obtained from high-pressure cylinders and flow rate was controlled using mass flow controllers. Steam was generated by supplying water from a high pressure syringe pump. Lines were heat traced to vaporize the water and preheat the feed gas. Valves in the sidearm permitted

flow rates to be established and diverted to vent while desired reaction conditions were achieved in inert $N_2$. Reactor product gases passed through a condenser and were vented through a back pressure regulator. During the test the sample weight was continuously monitored and the data was stored for further processing in the data acquisition system.

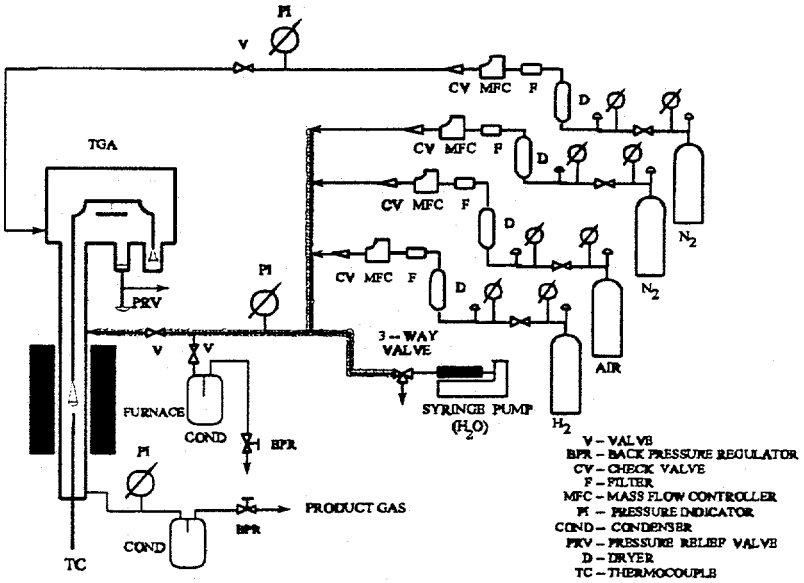


Figure 1. High Pressure Electrobalance Schematic

The raw data from the electrobalance is affected by aerodynamic drag and because of a time delay between switching the side-arm valve and the reactive gases contacting the sorbent. Delay time corrections, which depend on system volume between the side-arm valve and the sorbent, and flow rate, temperature, and pressure of the feed gas, were calculated on the basis of plug flow and applied to the raw data. The delay time varied from 0.12 to 2.94 minutes, depending on reaction conditions. Aerodynamic drag caused the apparent weight of the sample to be different from the true mass. Drag corrections as a function of temperature, pressure, and flow rate were experimentally determined under non-reacting conditions and also applied to the raw data.

**Time-Conversion Results**: Experimental time-conversion results including corrections for delay time and aerodynamic drag are shown in Figure 2 for a series of $O_2$ regeneration tests at 700°C, 5 atm, and 800 sccm total flow rate. Normalized sorbent mass, $M/M_o$, where $M_o$ is the initial mass, is plotted versus reaction time. The horizontal dashed line at $M/M_o = 0.909$ is the theoretical value corresponding to the complete regeneration of pure FeS to $Fe_2O_3$. The experimental final values of $M/M_o$ shown in Figure 2 range from 0.900 to 0.902. As will be seen, the final experimental values were generally in this range; the fact that they are smaller than theoretical is attributed primarily to impurities in the original FeS. The Figure 2 results show that the FeS-$O_2$ reaction is rapid at 700°C and is a strong function of $O_2$ concentration.

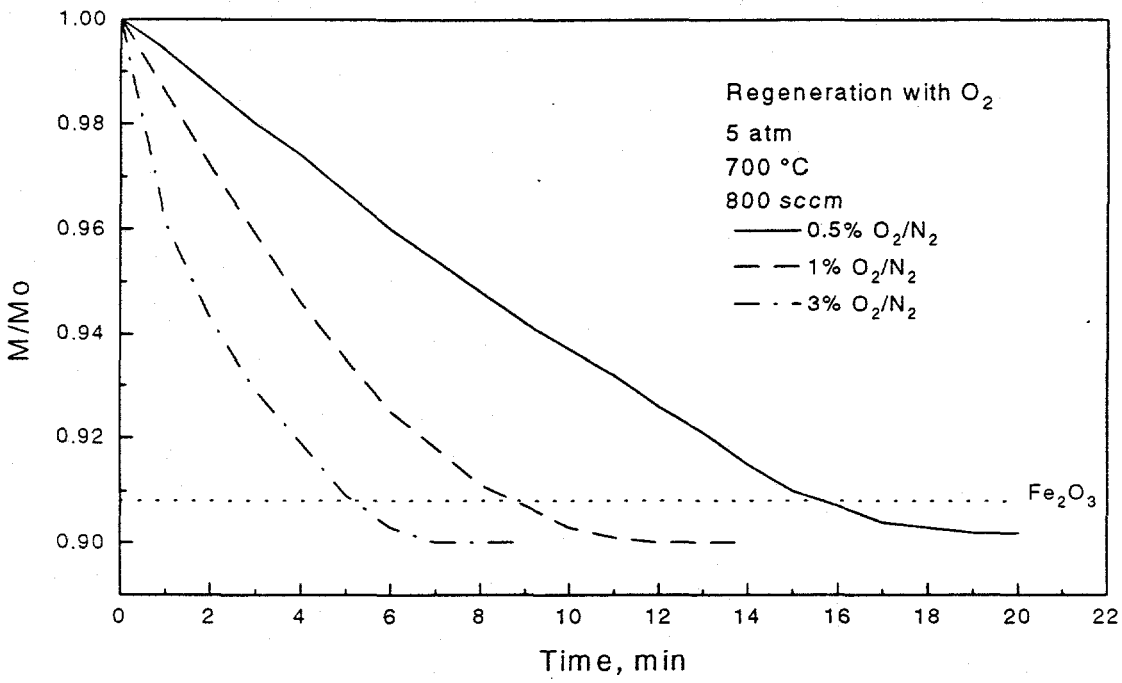


Figure 2. FeS Regeneration with $O_2$: The Effect of $O_2$ Concentration

Time-conversion results showing the effects of temperature and pressure are presented in Figures 3 and 4, respectively. In all cases the final normalized masses are slightly below theoretical. The effect of temperature, Figure 3, is shown at 5 atm using 1% $O_2$ at a feed gas rate of 800 sccm. The important result is the relatively small effect of temperature. Between 11 and 12 minutes were required for $M/M_o$ to reach the theoretical value of 0.0909 at 600°C while 7 to 8 minutes were required at 800°C. The effect of pressure is shown in Figure 4 at 700°C, 1% $O_2$ and a flow rate of 800 sccm. A relatively small increase in rate was observed in going from 1 to 5 atm, but the rate at 15 atm was slightly smaller than the 1 atm rate. This result was surprising since the $O_2$ concentration increased proportionally with pressure. The results shown in Figures 2 through 4 were typical of the results obtained at other reaction conditions.

Similar results for the FeS-$H_2O$ reaction showing the effect of $H_2O$ concentration, temperature, and pressure on the normalized mass versus time results are shown in Figures 5, 6, and 7, respectively. The horizontal dashed line in the figures at $M/M_o = 0.878$ corresponds to the stoichiometric value associated with complete conversion of FeS to $Fe_3O_4$. In these tests, there was greater scatter in the final values of $M/M_o$, with the experimental results being both above and below the stoichiometric value.

The reaction rate is a strong function of $H_2O$ mol fraction (Figure 5), just as the FeS-$O_2$ reaction. The temperature dependence of the FeS-$H_2O$ reaction (Figure 6) is somewhat greater than for the FeS-$O_2$ reaction, and the same unexpected effect of pressure was observed in both reactions. Figure 7 shows that the rate of the FeS-$H_2O$ reaction increased with pressure from 1 to 5 atm, but the rate at 15 atm was considerably smaller than the rate at 1 atm.

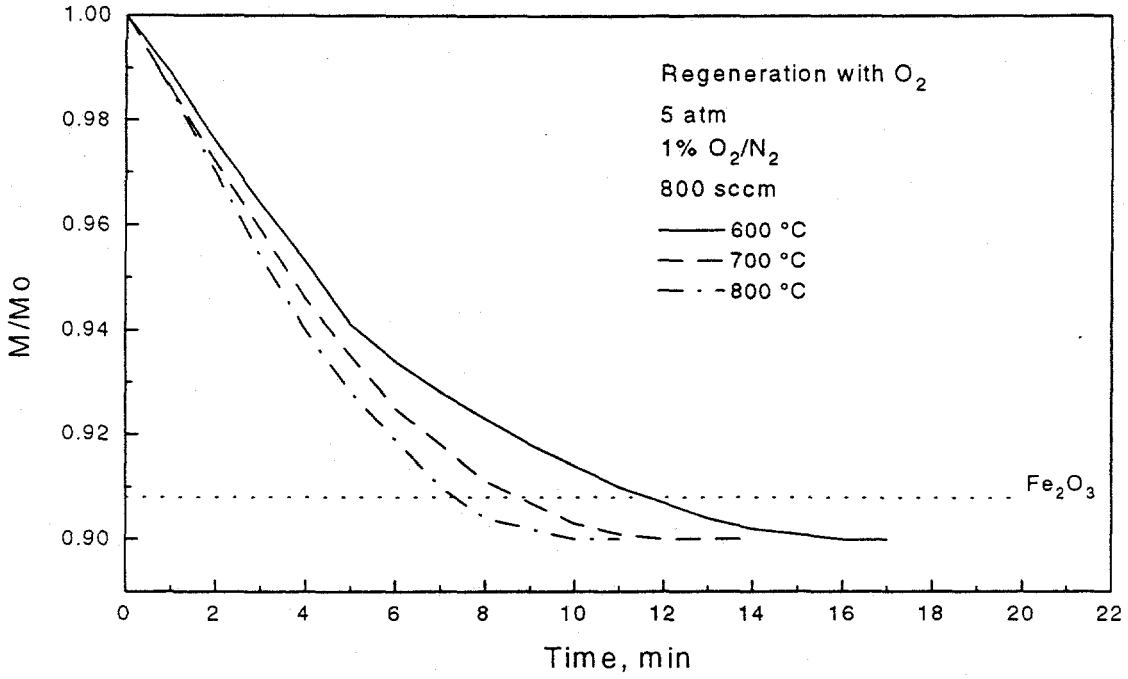


Figure 3. FeS Regeneration with $O_2$: The Effect of Temperature

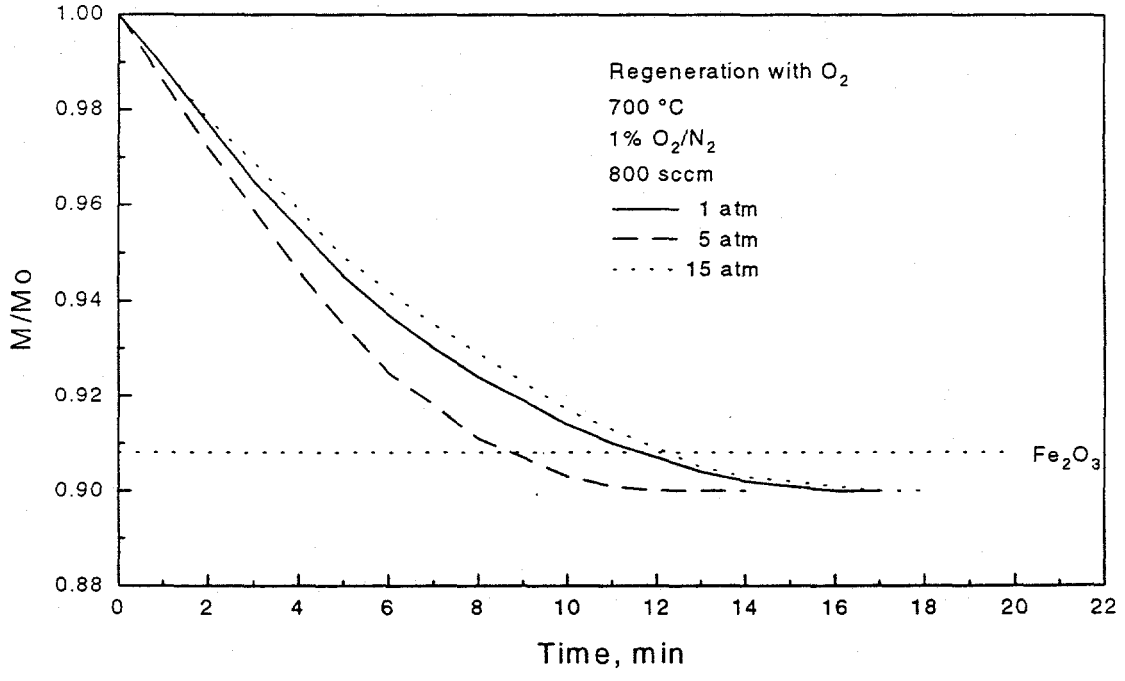


Figure 4. FeS Regeneration with $O_2$: The effect of Pressure

Comparison of the FeS-$O_2$ results (Figures 2 - 4) with the FeS-$H_2O$ results (Figures 5- 7) shows that FeS reacts much faster with $O_2$ than with $H_2O$. For example, at 700°C and 5 atm, approximately 18 minutes were required for complete regeneration in 0.5% $O_2$ (Figure 2) while almost 25 minutes were required for complete regeneration in 40% $H_2O$ at the same temperature and pressure (Figure 5).

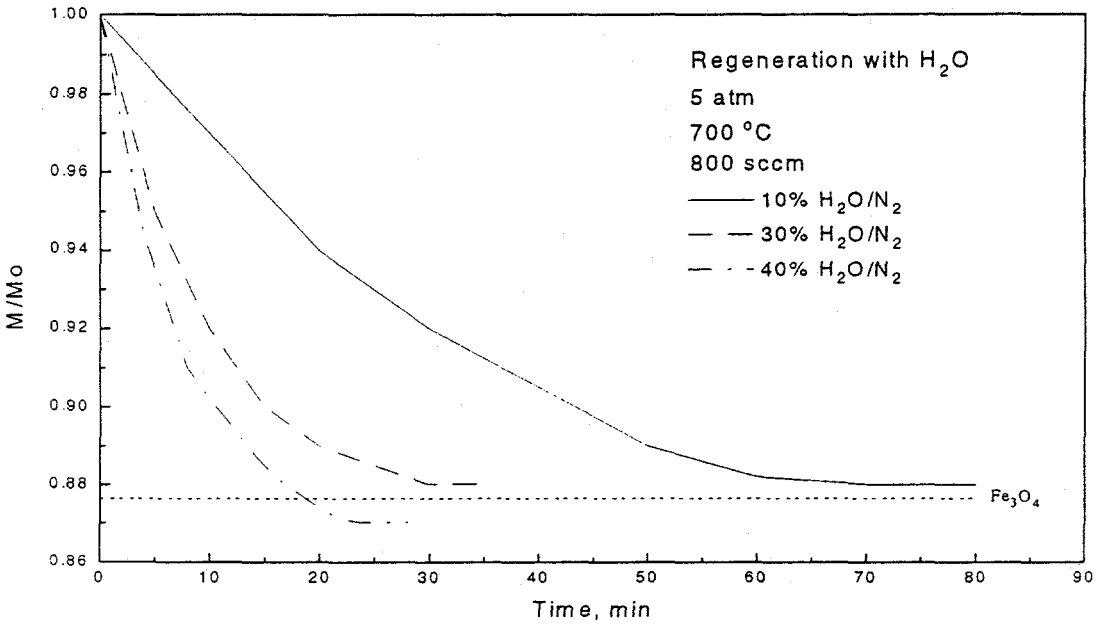


Figure 5. FeS Regeneration with $H_2O$: The Effect of $H_2O$ Concentration

A limited number of electrobalance tests were carried out in which the feed gas contained both $O_2$ and $H_2O$. The $H_2O$ content was held constant at 30% while the $O_2$ was varied from 0.05 to 0.5%. Normalized mass-time results as a function of $O_2$ content are shown in Figure 8. Horizontal dotted lines representing stoichiometric conversion to $Fe_2O_3$ and $Fe_3O_4$ are included in the figure. The final value of $M/M_o$ in all tests was slightly less than the stoichiometric value for $Fe_2O_3$ and was effectively equal to the value obtained in all FeS-$O_2$ tests. This was expected since any $Fe_3O$ formed by the FeS-$H_2O$ reaction should quickly be oxidized to $Fe_2O_3$ in the presence of $O_2$ via reaction (9).

The $H_2O/O_2$ ratio ranged from 60 to 600 in the tests shown in Figure 8. These ratios were sufficiently large that both the FeS-$O_2$ and FeS-$H_2O$ reactions contributed significantly to the total reaction rate. For example, from Figure 5 using 30% $H_2O$ and no $O_2$, about 30 minutes were required for complete reaction, compared to 10 minutes for complete reaction when 0.05% $O_2$ was added to the same $H_2O$ concentration (Figure 8). Similarly, from Figure 2, 18 minutes were required for complete reaction in 0.5% $O_2$ with no $H_2O$. This was reduced to the 8 minutes shown in Figure 8 when 30% $H_2O$ was added.

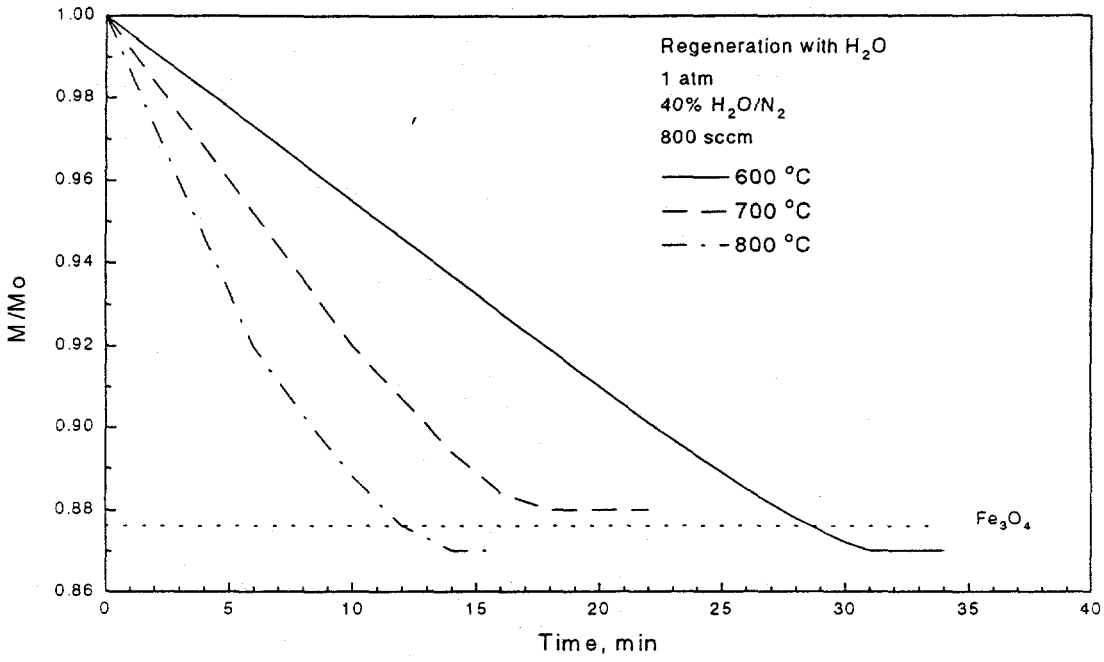


Figure 6. FeS Regeneration with $H_2O$: The Effect of Temperature

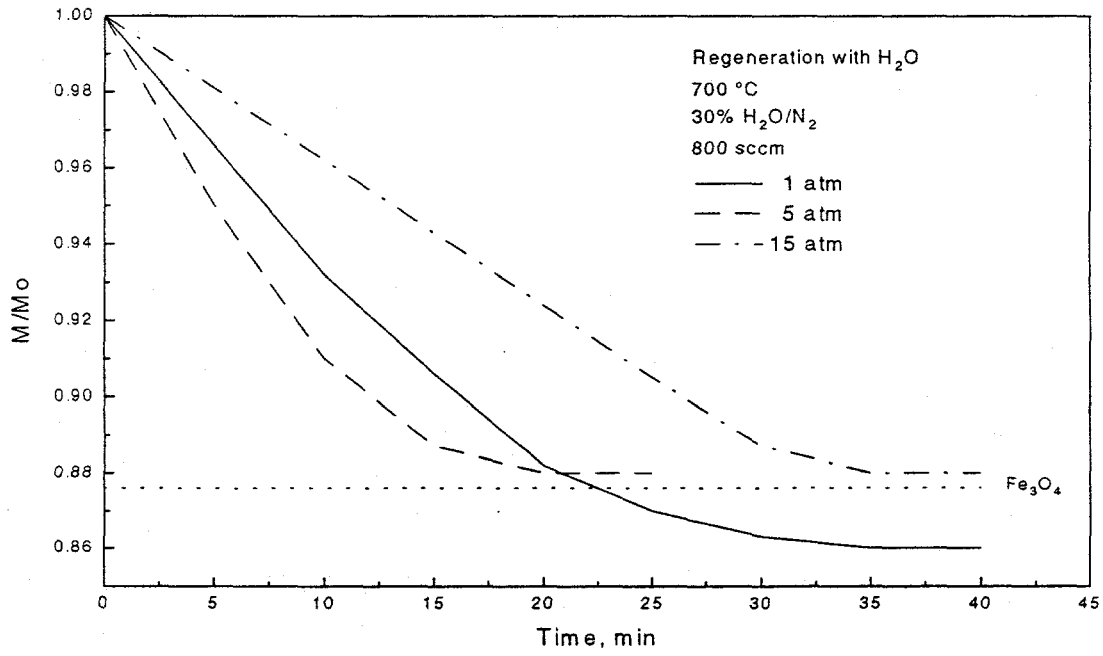


Figure 7. FeS Regeneration with $H_2O$: The Effect of Pressure

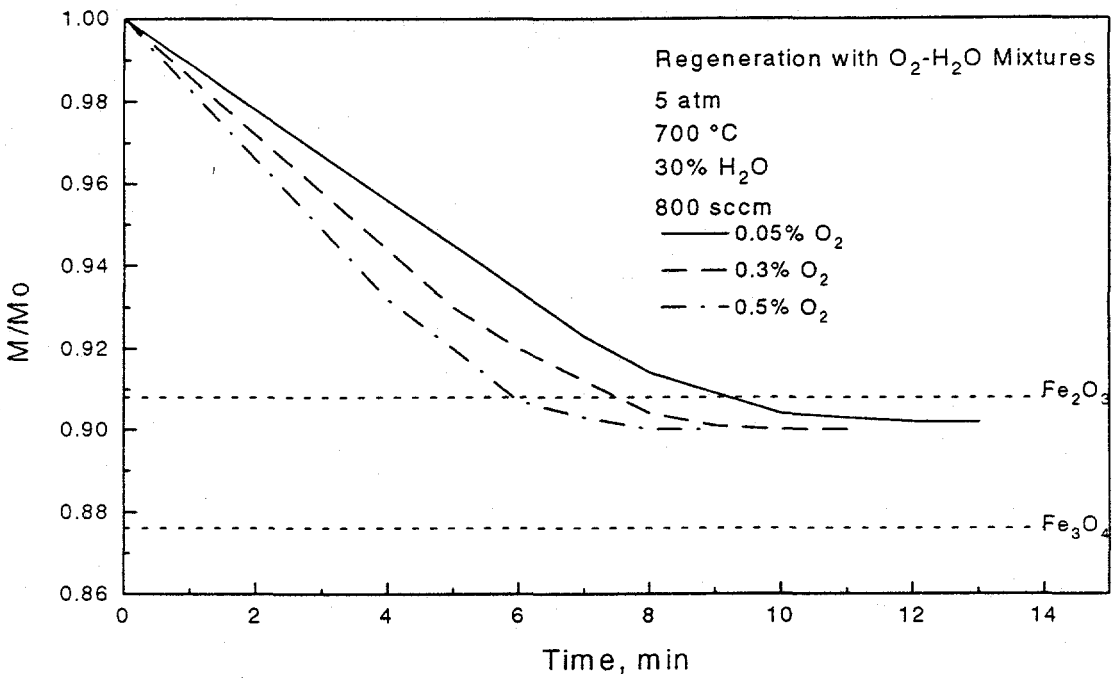


Figure 8. FeS Regeneration with $O_2$ and $H_2O$: The Effect of $O_2$ Concentration

The effects of temperature and pressure for the combined $O_2$-$H_2O$ reactions were qualitatively similar to those observed for the single reactions. An increase in temperature between 600 and 800°C resulted in a relatively small increase in the regeneration rate. The rate increased with pressure between 1 and 5 atm, but decreased to a minimum value at 15 atm.

## Fixed-Bed Reactor Studies

**Equipment**: A diagram of the fixed-bed reactor system is shown in Figure 9. The gas flow arrangement was similar to that used in the electrobalance reactor. Air and $N_2$ were obtained from high pressure cylinders and flow rates were controlled using mass flow controllers. Liquid water was fed using a high pressure syringe pump and downstream lines were heat traced to insure vaporization and to preheat the feed gases. The flow arrangement was such that $N_2$, $O_2$, and steam rates could be established and directed to vent while inert $N_2$ flowed through the reactor. Reactive gases were fed to the reactor by switching valve positions in the feed gas lines. The feed gases entered near the top of the reactor and flowed downward through the sorbent bed.

The sorbent was contained in an Alonized stainless steel insert within the pressure vessel. A porous quartz disc was supported on a ring welded into the insert. A layer of quartz wool was added above the disc and sorbent was placed above the quartz wool. High temperature O-rings at the top of the insert provided a seal between the insert and pressure vessel and prevented gas by-passing.

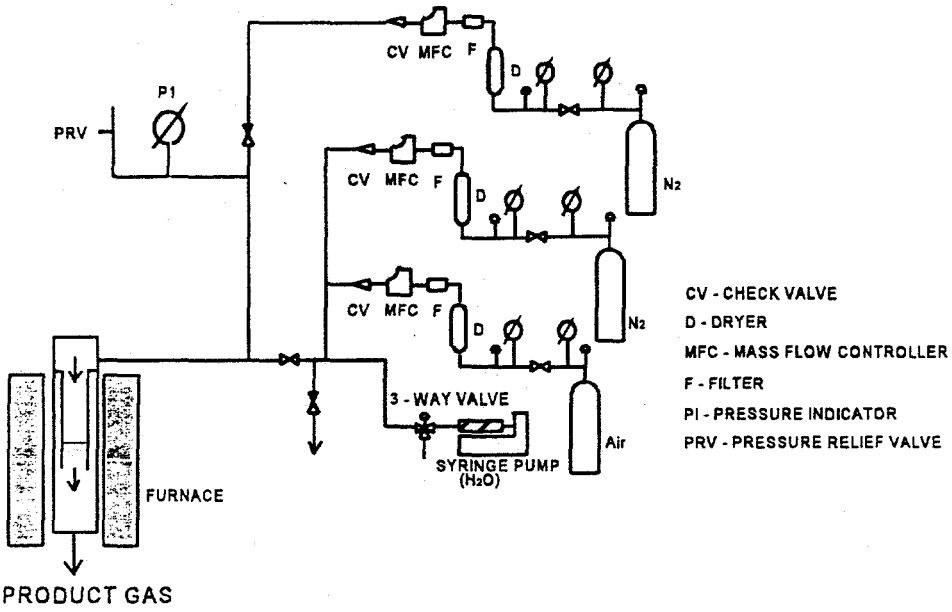


Figure 9. Fixed-Bed reactor schematic

Reactor product gases exited from the bottom of the reactor and entered the analytical system shown in Figure 10. Exit lines were maintained at high temperature to prevent elemental sulfur condensation. The product gas was split into two steams, with one portion flowing through a capillary flow restrictor into an oxidation chamber at 1050°C where all sulfur compounds were converted to $SO_2$. Excess $H_2O$ was removed using a membrane dryer and total sulfur concentration was determined using a calibrated UV-Fluorescence detector. Flow through this portion of the analytical system was determined by the reactor pressure and the resistance of the capillary restrictor. As might be excepted, this system proved to be quite troublesome and frequent recalibration was necessary. The primary problem was caused by the resistance of the restrictor varying due to particulate carryover from the reactor.

The remainder of the product gas entered the bottom leg of the analytical system and passed through a condenser and series of filters where elemental sulfur was separated from the permanent gases. $H_2S$ and $SO_2$ concentrations were then determined by gas chromatography. Although the technique involved the determination of elemental sulfur by difference (total sulfur- $H_2S$-$SO_2$), it provided reasonable accuracy when the concentration of elemental sulfur was sufficiently large.

**Experimental Results**: Reaction conditions associated with each of the experimental runs described in this report are presented in Table 2. Pressure was constant at 4.4 atm while temperature varied between 550 and 700°C. The regeneration feed gas contained from 0 to 1.5% $O_2$, 0 to 52% $H_2O$, and balance $N_2$. In runs in which the feed gas contained both $H_2O$ and $O_2$, the $H_2O/O_2$ ratio ranged from 6.7 to 200. The sorbent bed consisted of a physical mixture of FeS and $Al_2O_3$, with the quantity of FeS varied in relation to the feed gas flow rate and $O_2$ content to insure complete regeneration in a reasonable time. Volumetric feed rate ranged from 300 to 600 sccm. Reaction conditions, in

particular temperature and feed gas composition, were selected on the basis of the electrobalance test results.

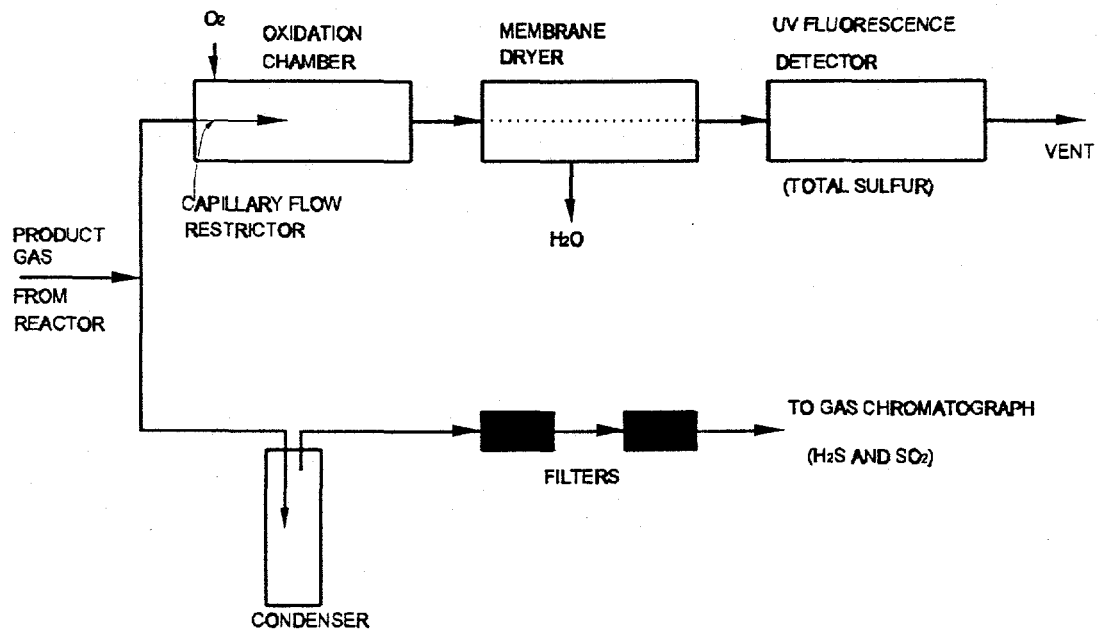


Figure 10. Product Gas Analytical System

With $O_2$ as the only reactive component in the feed gas, all sulfur should be liberated as $SO_2$ according to reaction (6). Experimental results from run FeS-11, expressed as mol fraction $SO_2$ in the product gas as a function of dimensionless time are shown in Figure 11. Dimensionless time is defined so that $t^* = 1$ would correspond to complete regeneration of FeS and complete conversion of $O_2$ if the reaction occurred at an infinitely fast rate. After a brief delay at the beginning of the run, the $SO_2$ concentration increased quickly to about 0.0085 mol fraction and was approximately constant until the reaction neared completion. The FeS-$O_2$ reaction was quite rapid as indicated by the steepness of the $SO_2$ concentration decrease near the end of the run, and the facts that the "steady-state" $SO_2$ concentration was near the stoichiometric value corresponding to complete $O_2$ consumption (indicated by the dashed horizontal line) and that the reaction was almost complete at $t^* = 1.0$.

When the feed gas contained only $H_2O$, all sulfur was liberated as $H_2S$ according to reaction (7). In agreement with electrobalance test results, this reaction was quite slow as shown by the results of run FeS-14 in Figure 12. The steady-state $H_2S$ concentration was only about 1.7% of the stoichiometric maximum, and regeneration was only 12% complete when the run was terminated after eight dimensionless time steps. The greater scatter in the data is attributed to the difficulty in maintaining a constant steam flow rate.

Table 2. Reaction Conditions for FeS Partial Oxidation Regeneration

| Run | FeS-04 | FeS-11 | FeS-14 | FeS-16 | FeS-19 | FeS-22 | FeS-25 | FeS-26 |
|---|---|---|---|---|---|---|---|---|
| Sorbent Mass, g | | | | | | | | |
| FeS | 1.73 | 3.27 | 3.22 | 3.21 | 0.83 | 0.83 | 0.50 | 0.83 |
| $Al_2O_3$ | 3.04 | 3.29 | 3.21 | 3.27 | 3.28 | 3.28 | 3.80 | 3.29 |
| Temperature, °C | 550 | 600 | 700 | 700 | 700 | 600 | 600 | 600 |
| Pressure, atm | 4.4 | 4.4 | 4.4 | 4.4 | 4.4 | 4.4 | 4.4 | 4.4 |
| Feed Gas Composition, mol% | | | | | | | | |
| $O_2$ | 0.5 | 1.5 | 0 | 1.5 | 0.25 | 0.25 | 0.26 | 0.25 |
| $H_2O$ | 23.3 | 0 | 10.0 | 10.0 | 20.0 | 20.0 | 52.0 | 20.0 |
| $N_2$ | 76.2 | 98.5 | 90.0 | 88.5 | 79.75 | 79.75 | 47.74 | 79.75 |
| $H_2O/O_2$ | 47 | -- | -- | 6.7 | 80 | 80 | 200 | 80 |
| Feed Gas Rate, sccm | 300 | 600 | 600 | 600 | 300 | 300 | 435 | 600 |

When the feed gas contains both $O_2$ and $H_2O$, reactions (8) and (9) also become important. The formation of elemental sulfur by the Claus reaction depends on the relative quantities of $SO_2$ and $H_2S$ and the position within the sorbent bed where they are formed. There must be sufficient $H_2S$-$SO_2$ contact time for the Claus reaction to occur.

Results from run FeS-22 in which the feed gas contained $H_2O$ and $O_2$ in a 80-to-1 ratio are shown in Figure 13. The mol factions of $SO_2$ and $H_2S$ determined by gas chromatography and total sulfur determined by the UV-fluorescence detector are plotted versus dimensional time. Dimensional time is used since dimensionless time cannot be clearly defined when multiple reactions occur. After a brief delay, both the total sulfur and $H_2S$ concentrations increased rapidly with the total sulfur reaching a maximum of 0.0025 mol fraction after 0.9 hours and the $H_2S$ maximum of 0.00065 mol fraction occurring after 1.7 hours. $SO_2$ concentration was effectively zero during the first hour and then gradually increased to a maximum of 0.00072 after six hours. After reaching their maxima, the concentrations of all species decreased gradually. The $H_2S$ mol fraction approached zero after 5.1 hours and the total sulfur and $SO_2$ concentrations approached zero after eight hours.

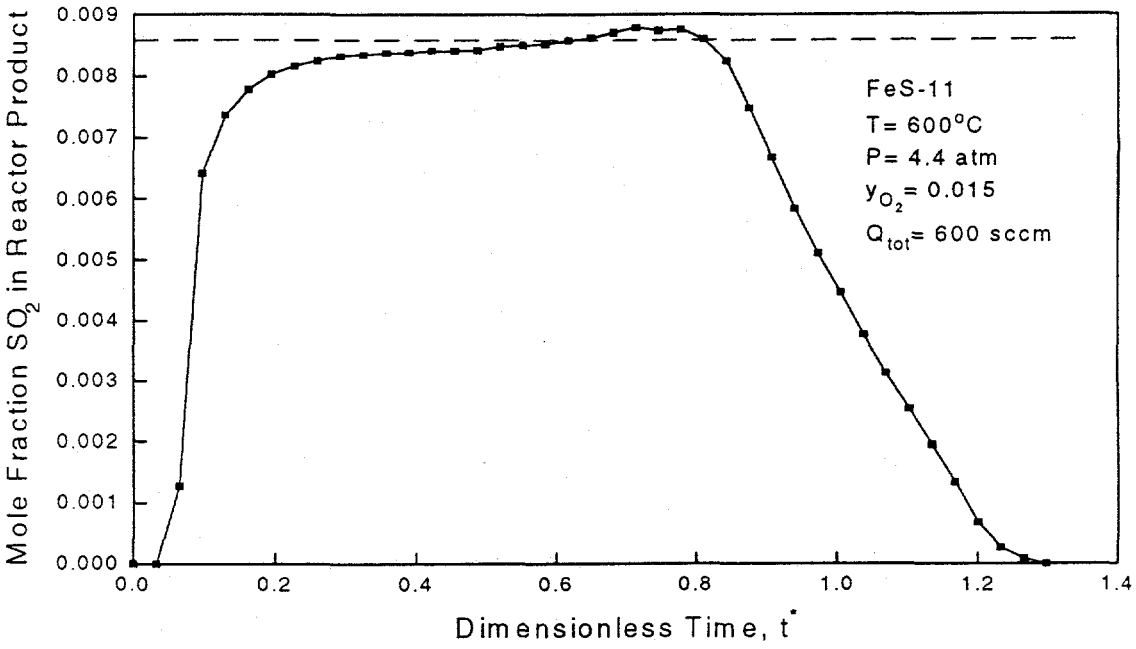


Figure 11. Fixed-Bed Reactor Response: $H_2O$ regeneration, Run FeS-14

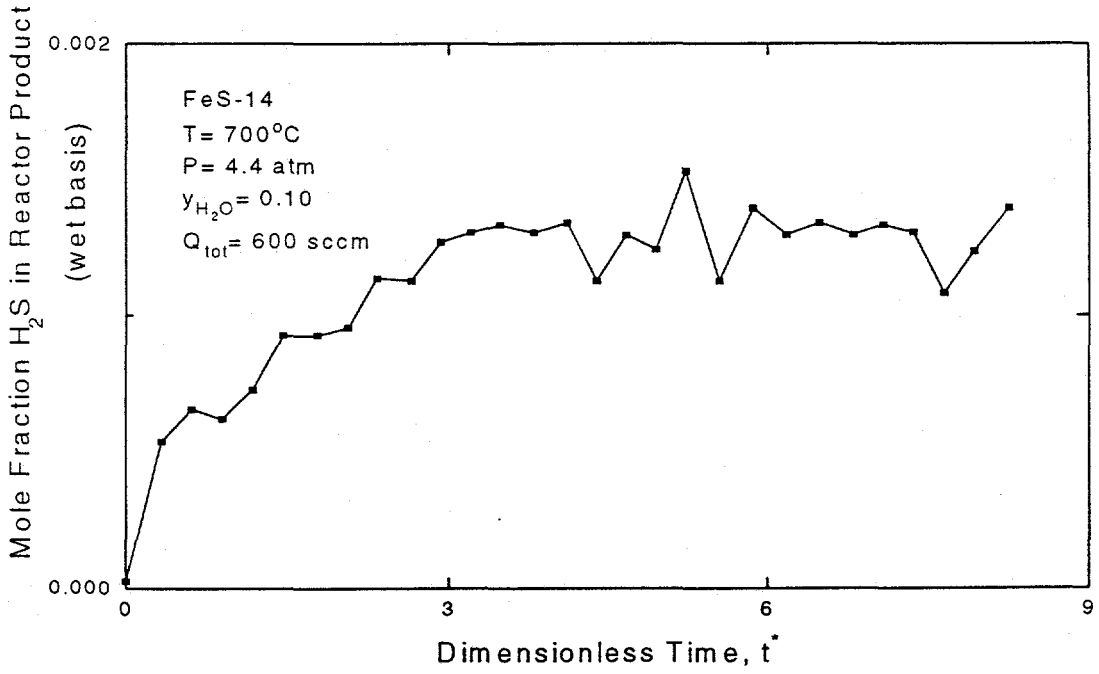


Figure 12. Fixed-Bed Reactor response: $H_2O$ Regeneration, Run FeS-14

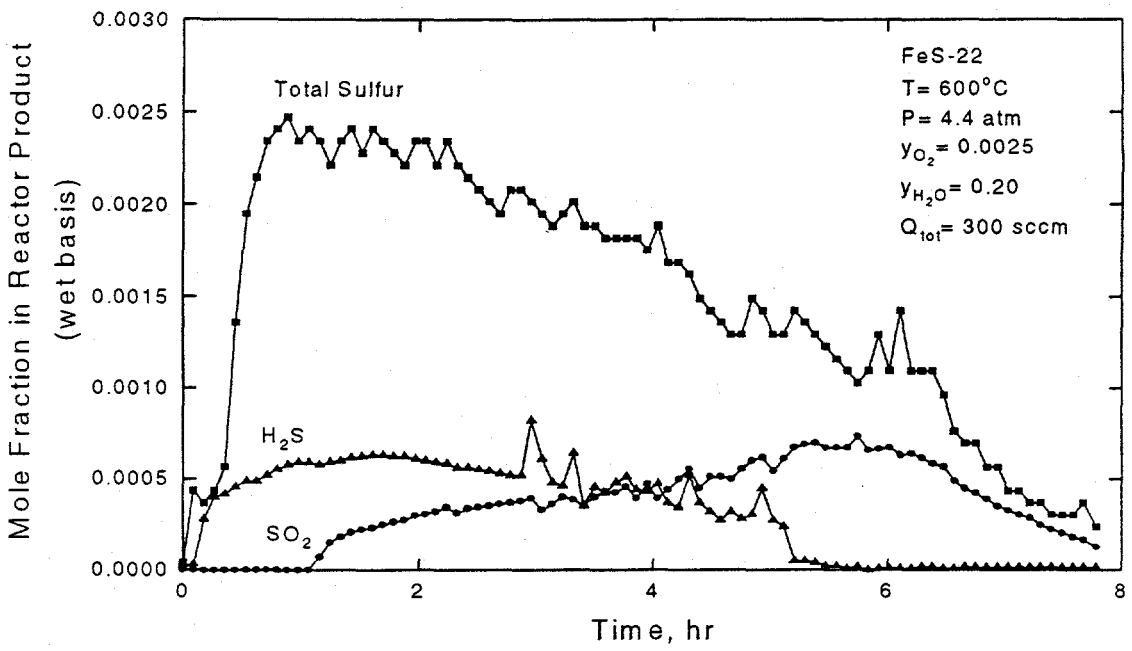


Figure 13. Fixed-Bed Response: $H_2O$ and $O_2$ Regeneration, Run FeS-22

The cumulative production of each sulfur species as a function of time was determined by numerical integration of the concentration-time data. The cumulative amounts produced at the end of the reaction provided a check on the overall sulfur material balance. Results of the numerical integration of the run FeS-22 data are shown in Figure 14. The production of $H_2S$, $H_2S+SO_2$, and total sulfur, all expressed as a fraction of the theoretical sulfur associated with the initial FeS charge, are plotted versus reaction time. After the brief time delay, the amount of $H_2S$ gradually increased to account for about 21% of the theoretical sulfur after 5.1 hours; no more $H_2S$ was produced after that time. The $H_2S$ and $H_2S+SO_2$ curves coincided for the first hour when no $SO_2$ was produced. Thereafter, the curves diverged and the cumulative production of $H_2S+SO_2$ was 45% of theoretical by the end of the run; this corresponds to cumulative $SO_2$ production of 24% of theoretical. The overall sulfur material balance for this run was quite good as the cumulative production of total sulfur by the end of the run was 99% of theoretical. Thus, about 55% of the sulfur was liberated in elemental form.

The instantaneous selectivity of elemental sulfur in run FeS-22 is shown in Figure 15. Selectivity is defined by

$$S(t) = \frac{Elemental\ Sulfur}{Total\ Sulfur} = \frac{Total\ Sulfur - (SO_2 + H_2S)}{Total\ Sulfur}$$

Although there is significant scatter in the results, particularly near the beginning and end of the run where $H_2S + SO_2$ concentration is approximately equal to total sulfur concentration, there is a clear trend to the data. Near the beginning, about 80% of the sulfur was released in elemental form. This was followed by a more or less linear decrease to near 20% at the end of the run. The cumulative, or time average, selectivity was, as shown in Figure 14, about 55%.

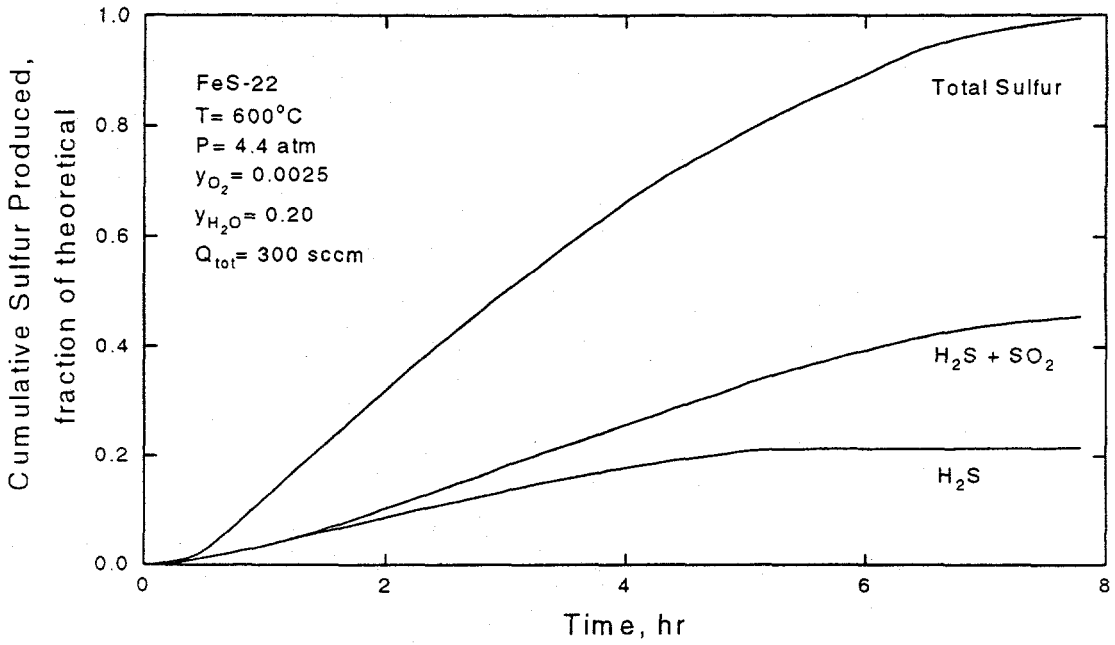


Figure 14. Cummulative Production of $H_2S$, $H_2S+SO_2$, and Total Sulfur, Run FeS-22

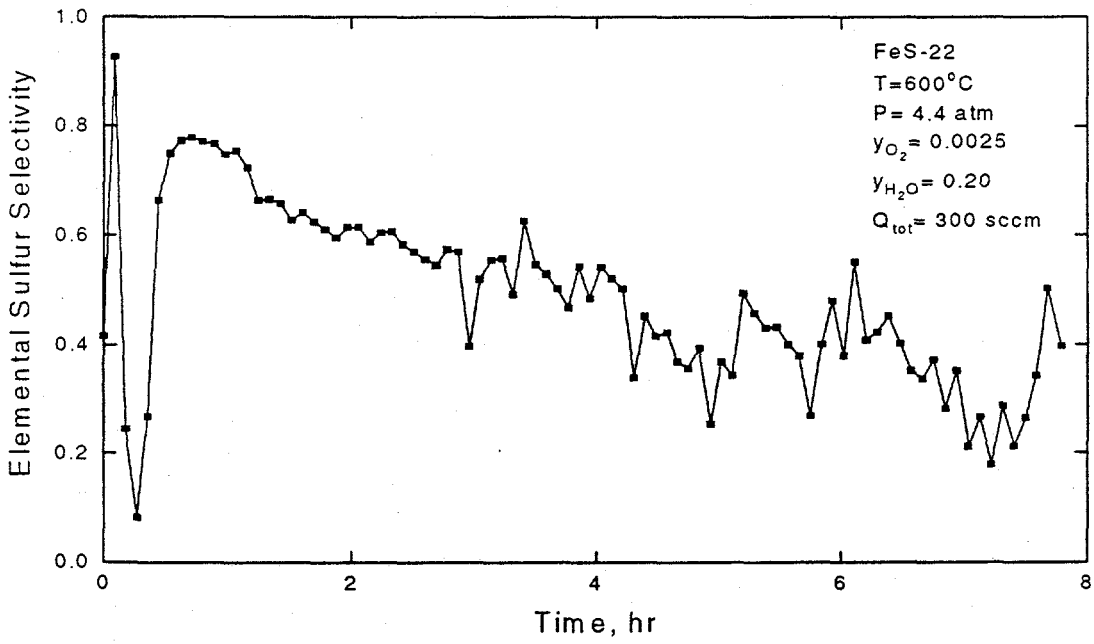


Figure 15. Instantaneous Selectivity to Elemental Sulfur, Run FeS-22

Maximum elemental sulfur selectivity occurred at low temperature, small regeneration gas flow rate, and large $H_2O$-to-$O_2$ ratio. The minimum temperature for complete regeneration was about 600°C. At lower temperatures, for example at 550°C used in run FeS-04, regeneration was incomplete, presumably because stable $Fe_2(SO_4)_3$ was formed. However, there was no indication of $Fe_2(SO_4)_3$ at 600°C or above, as shown by the results of run FeS-22.

Concentration-time results from run FeS-19 at the higher temperature of 700°C are shown in Figure 16. Reaction conditions other than temperature were identical in runs FeS-19 and FeS-22. The concentration-time responses were qualitatively similar as were the total run duration, maximum concentration of total sulfur, and the time corresponding to the total sulfur maximum. However, the maximum $SO_2$ concentration was about 50% larger at the higher temperature and the maximum occurred at an earlier time. The largest differences was associated with $H_2S$ where maximum concentration doubled and the time corresponding to the maximum was reduced by about 25%. Numerical integration showed that only about 40% of the sulfur in run FeS-19 was released in elemental form.

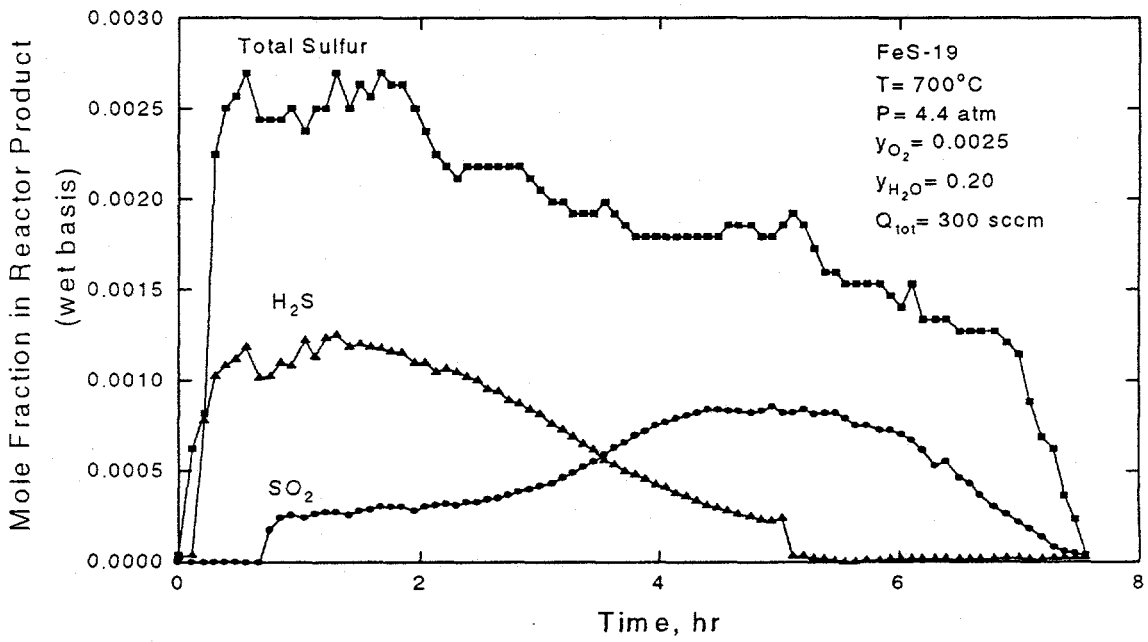


Figure 16. Fixed-Bed Reactor Response: $H_2O$ and $O_2$ regeneration, Run FeS-19

Doubling the regeneration gas feed rate from 300 sccm in run FeS-22 to 600 sccm in FeS-26, while keeping other regeneration conditions constant, had a moderate negative effect on elemental sulfur production. The $H_2S$ and $SO_2$ responses with time were similar to those shown in Figures 13 and 16, but the maxima were at larger mol fractions. Slightly less than 50% of the sulfur was liberated in elemental form in run FeS-26 compared to 55% in FeS-22. Varying the $H_2O$-to-$O_2$ ratio produced the largest effect on elemental sulfur selectivity. This may be seen by comparing the concentration-time results of run FeS-16 using a $H_2O$-$O_2$ ratio of 6.7 (Figure 17) and run FeS-25 using a $H_2O$-$O_2$ ratio of 200 (Figure 18) with the results from run FeS-22 at a $H_2O$-$O_2$ ratio of 80

(Figure 13). At small $H_2O$-$O_2$ ratio, as shown in Figure 17, the sum of the $H_2S$ and $SO_2$ concentrations was approximately equal to the total sulfur concentration, indicating that the amount of elemental sulfur produced was quite small. Although the higher temperature and larger feed rate in run FeS-16 also contributed to reduced elemental sulfur formation, these effects were insufficient to explain the almost total absence of elemental sulfur.

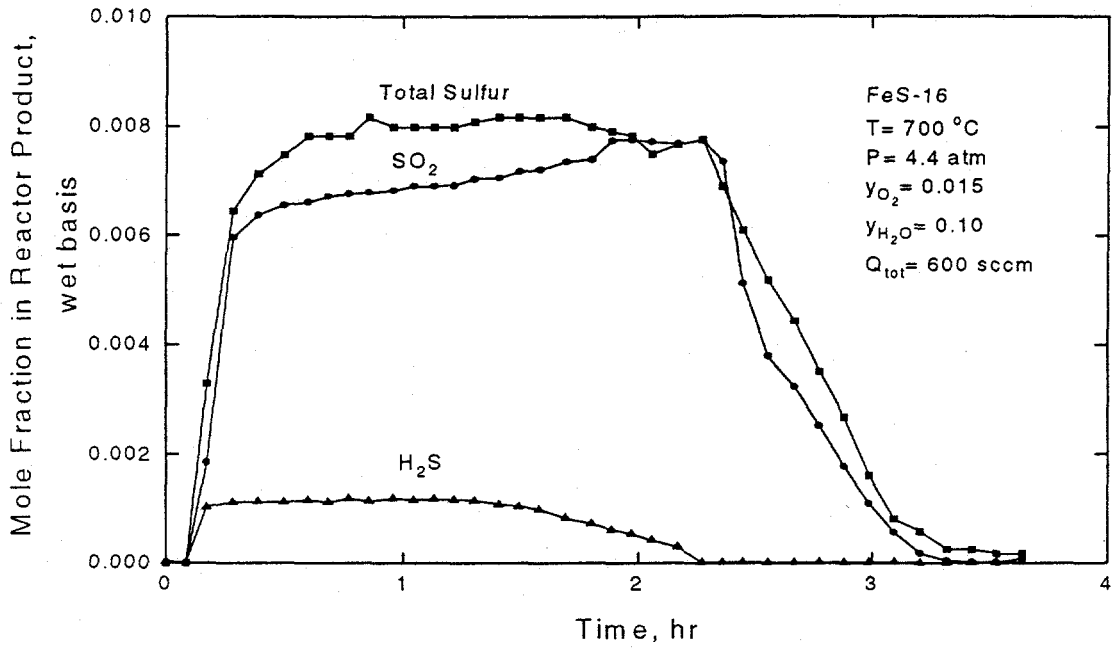


Figure 17. Fixed-bed Reactor response: $H_2O$ and $O_2$ Regeneration, Run FeS-25

When the $H_2O$-$O_2$ ratio was increased to 200 in run FeS-25 (Figure 18), the cumulative elemental sulfur selectivity increased to 75%. Although the feed rate in FeS-25 was somewhat larger than in FeS-22, the larger feed rate should, based on previous discussion, reduce the elemental sulfur yield. With the exception of the large early peak in total sulfur concentration, the results in Figure 18 are qualitatively similar to other time-conversion results. The cumulative yields of $H_2S$ and $SO_2$ in FeS-25 were only 15% and 10% of theoretical, respectively, and about 75% of the sulfur was liberated in elemental form.

## Interpretation

The results of the FeS regeneration tests may be interpreted on the basis of reactions (6) through (9). Consider Figure 19a which shows proposed solid and gas concentration profiles within the sorbent bed during the early stages of the reaction, corresponding to just less than one hour in run FeS-22 (Figure 13). Because of the large rate of the FeS-$O_2$ reaction, the reaction interface separating $Fe_2O_3$ and FeS is quite steep. Only a small amount of $Fe_3O_4$, as indicated by the almost horizontal line extending from the FeS-$Fe_2O_3$ interface to the reactor exit, is present because the FeS-

$H_2O$ reaction is slow. $Fe_3O_4$ will exist only downstream of the $Fe_2O_3$-FeS interface since $Fe_3O$ will be quickly oxidized to $Fe_2O_3$ when contacted by $O_2$.

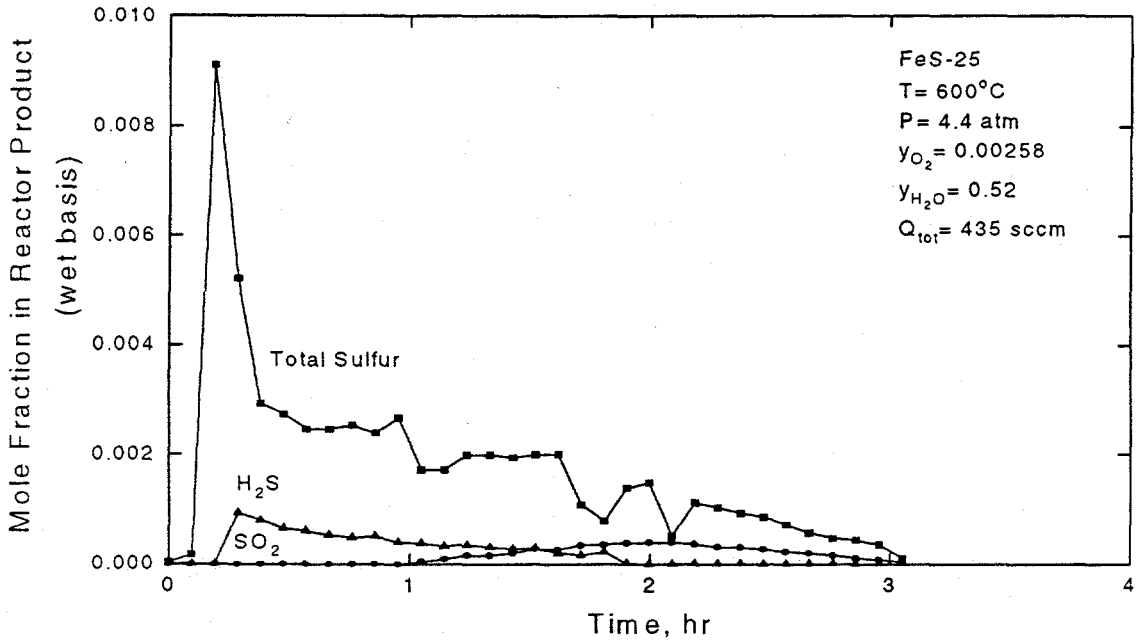


Figure 18. Fixed-Bed Reactor Response: $H_2O$ and $O_2$ Regeneration, Run FeS-25

The shape of the $O_2$ concentration profile is approximately equivalent to the $Fe_2O_3$-FeS interface, but with minimal distortion due to the additional consumption of $O_2$ in converting $Fe_3O$ to $Fe_2O_3$. Inlet $H_2O$ concentration is much larger than inlet $O_2$ concentration (the $H_2O$-$O_2$ ratio in run FeS-22 is 80) and no $H_2O$ reacts upstream of the $Fe_2O_3$-FeS interface. Downstream of the interface there is a small, almost linear, decrease in the $H_2O$ concentration.

Proposed $SO_2$ and $H_2S$ concentration profiles in the absence of the Claus reaction (reaction (8)) are shown by the solid lines in Figure 19a. The $SO_2$ concentration profile is quite steep and rises to a value equal to 57% of the inlet $O_2$ concentration as specified by reaction (6). The $H_2S$ concentration is zero to the position of the $Fe_2O_3$-FeS interface and increases almost linearly from there to the bed exit. The final $H_2S$ concentration is equal to 75% of the change in $H_2O$ concentration according to reaction (7). At positions within the reactor where $SO_2$ and $H_2S$ co-exist, elemental sulfur may be formed by the Claus reaction (8), and $SO_2$ and $H_2S$ concentration profiles are modified as shown by the dotted lines in Figure 19a. No additional $SO_2$ may be formed downstream of the $Fe_2O_3$-FeS interface where the $O_2$ concentration is zero. Hence, the $SO_2$ concentration reaches a maximum at some interior bed position and decreases thereafter. In contrast, no $H_2S$ is formed upstream of the $Fe_2O_3$-FeS interface, and additional $H_2S$ is formed downstream of the point where the $SO_2$ concentration is zero.

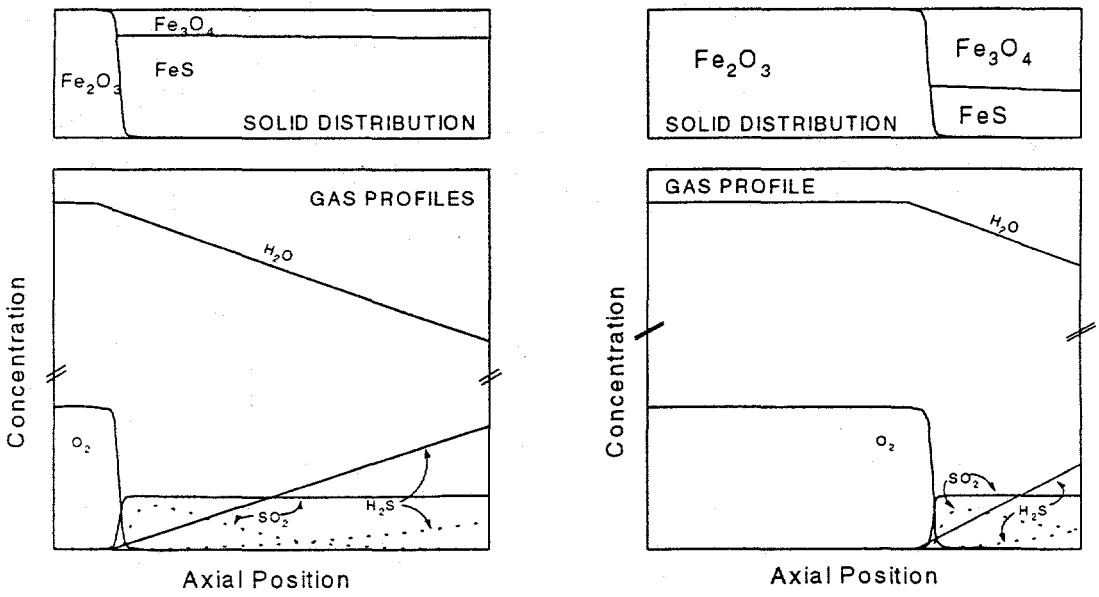


(a) at an Early Stage of the Reaction (b) at an Intermediate Stage of the Reaction

Figure 19. Proposed Solids Distribution and Gas Concentration Profiles within the Sorbent Bed

The quantity of $SO_2$ formed within the bed is almost independent of time prior to $O_2$ breakthrough. The only difference is the axial position at which the $SO_2$ is produced. In contrast, the quantity of $H_2S$ formed is a maximum initially and decreases continuously with time as the $Fe_2O_3$-FeS interface moves through the bed. The maximum amount of $H_2S$ coupled with the maximum contact time between $SO_2$ and $H_2S$ is responsible for the elemental sulfur selectivity being maximum initially and decreasing with time. Because the fixed quantity of $SO_2$ contacts the maximum amount of $H_2S$ for the maximum amount of time during the early stages of the reaction, all of the $SO_2$ reacts which leads to zero $SO_2$ product gas concentration. $H_2S$ product concentration is not zero, however, since additional $H_2S$ is formed downstream of the point where the $SO_2$ concentration is zero.

As the reaction progresses, the $Fe_2O_3$-FeS interface moves further into the bed and the concentration profiles are modified as shown in Figure 19b. These profiles correspond to a reaction time of about 4 hours in run FeS-22 (Fig. 13). The shape of the $Fe_2O_3$-FeS interface is similar to that at the earlier time, but displaced to the right. Again, no $Fe_3O_4$ exists to the left of the $Fe_2O_3$-FeS interface. To the right of the interface, the $Fe_3O_4$ profile remains almost horizontal but the concentration is increased due to the increased reaction time. The $O_2$ concentration profile is also similar to the earlier $O_2$ profile, but displaced to the right. The $H_2O$ profile remains flat, but even less $H_2O$ reacts because of the reduced contact time downstream of the $Fe_2O_3$-FeS interface. In the absence of the Claus reaction, the $SO_2$ concentration profile (solid line) is unchanged except for downstream position. The $H_2S$ profile (solid line) is also similar, but initial $H_2S$ formation is delayed because of the shift in the $Fe_2O_3$-FeS interface and the final $H_2S$ concentration is smaller because of the reduced reaction time. When the Claus reaction is present (dashed lines), less $SO_2$ is consumed because less $H_2S$ is present and the contact time is less. Therefore, both $SO_2$ and $H_2S$ appear in the product gas.

The effects of flow rate, temperature, and $H_2O/O_2$ ratio on elemental sulfur production are consistent with the above interpretation. Doubling the feed gas rate from 300 to 600 sccm (runs FeS-22 and FeS-26) increased the selectivity to $SO_2$, had little effect on H Ş selectivity, and, as a consequence, reduced the elemental sulfur selectivity. The increased flow rate caused no change in the $SO_2$ production rate. However, less $H_2S$ was formed due to the reduced residence time, and there was less time for the Claus reaction to occur. These effects tended to cancel to produce essentially no change in $H_2S$ production, and left more $SO_2$ and less elemental sulfur in the product.

Higher temperature, in contrast, increased the $H_2S$ yield, had little effect on the amount of $SO_2$ produced, and caused the elemental sulfur selectivity to decrease. This is consistent with the electrobalance results which showed that the FeS-$H_2O$ reaction was more sensitive to temperature than the FeS-$O_2$ reaction (compare Figures 3 and 6). Although more $H_2S$ was formed, much of it was formed downstream of the $Fe_2O_3$-FeS reaction front and had less opportunity to react with $SO_2$.

The strong effect of $H_2O/O_2$ ratio on elemental sulfur selectively, which ranged from almost zero at a ratio of 6.7 (Figure 17) to about 75% at a ratio of 200 (Figure 18), is also due to the large difference in the reaction rates of FeS with $O_2$ and $H_2O$. Large elemental sulfur selectivity requires that a large fraction of the FeS react with $H_2O$ to liberate $H_2S$, and, of equal importance, that both $H_2S$ and $SO_2$ be formed at positions within the bed which provides sufficient time for the Claus reaction to occur. $H_2S$ formed near the exit of the bed is swept out of the reactor without having a chance to be converted to elemental sulfur.

### Summary

While reasonably large selectivities to elemental sulfur are possible at large $H_2O/O_2$ ratios, the elemental sulfur concentration in the product gas was always quite small and the relatively low temperature required to condense the sulfur would result in the condensation of large quantities of steam. The large steam requirement and the large heat duty of the sulfur condenser, coupled with the difficulty of handling the sulfur and water mixture, are believed to make this concept impractical.

## CERIUM OXIDE STUDIES

Regeneration of cerium oxysulfide, $Ce_2O_2S$, which is the product of the reaction between $CeO_2$ and $H_2S$ was chosen for the second phase of the exploratory test series. Since $Ce_2O_2S$ is not available commercially, it was necessary to carry out both the sulfidation and regeneration reactions. However, primary emphasis in the exploratory phase was given to the regeneration step. $SO_2$ served as the oxidizing agent in regeneration. The important reactions are

$$2CeO_2(s) + H_2S(g) + H_2(g) ==> Ce_2O_2S(s) + 2H_2O(g) \quad (10)$$

$$Ce_2O_2S(s) + SO_2(g) ==> 2CeO_2(s) + S_2(g) \quad (11)$$

**Fixed-Bed Reactor**

Only minor modifications to the fixed-bed reactor system shown in Figure 9 were required. The sulfidation gas consisted of $H_2S$, $H_2$, and $N_2$ while $SO_2$ and $N_2$ mixtures were used in the regeneration studies. Flow rates of these gases were controlled by mass flow controllers. The room temperature vapor pressures of $H_2S$ and $SO_2$ limited the sulfidation and regeneration pressures to 5 atm and 1 atm, respectively.

Product gas exited from the bottom of the reactor, and, after flowing through a condenser, a sequence of filters, and a back pressure regulator, the composition was determined by gas chromatography. The exit line between the reactor and condenser was heat traced to minimize condensation of elemental sulfur during the regeneration tests.

The gas chromatograph was equipped with a thermal conductivity detector which measured $H_2S$ concentration during sulfidation tests and $SO_2$ concentration during regeneration, both as a function of time. Since both the sulfidation and regeneration reactions were stoichiometrically "clean," it was not necessary to use the total sulfur analyzer, which greatly simplified the analysis compared to the FeS partial oxidation regeneration tests.

Initial sulfidation tests were plagued with "over-sulfidation," that is, the apparent amount of $H_2S$ removed greatly exceeded the stoichiometric quantity associated with the conversion of $CeO_2$ to $Ce_2O_2S$. The formation of $Ce_2S_3$ instead of $Ce_2O_2S$ was initially suspected as the cause of the over sulfidation. This explanation was later rejected when increasing the oxygen content of the feed gas (by the addition of $CO_2$ and/or $H_2O$) did not alter the result. Reaction between $H_2S$ and the walls of the stainless steel insert was later determined to be the cause of "over-sulfidation." Although the insert had been Alonized to prevent reaction, it was either ineffective at the 800°C temperature used for most $CeO_2$ sulfidation tests or had deteriorated during the FeS regeneration studies to the point that protection was no longer provided.

The problem was ultimately solved by replacing the stainless steel insert with a quartz insert shown in Figure 20. While not totally eliminating contact between $H_2S$ and high temperature steel surfaces, contact was minimized to the point that sulfur material balance closure in subsequent sulfidation tests has typically been within ±10% of stoichiometric. The quartz insert is attached to the top of the pressure vessel by a stainless steel ring and o-rings which fit over the shoulders at the top of the insert. These o-rings do not provide a pressure seal, but prevent gas by-passing and supply a flexible cushion to accommodate differences in the thermal expansion coefficients between the quartz and stainless steel. Dimples located near the bottom of the insert within the isothermal zone of the furnace support a porous quartz disk, a layer of quartz wool, and then the sorbent. The fragility of the quartz insert requires that extreme care be exercised when loading and unloading sorbent and assembling and disassembling the reactor. However, the arrangement has proven to be quite reliable and only one breakage has occurred during operation.

The primary operational problem has been caused by elemental sulfur plugging the tubing and filters between the reactor and chromatograph. As previously stated, the reactor product gas passes through a length of heated tubing into a condenser where most of the sulfur is removed and then through a sequence of filters before entering the chromatograph. The condenser contains quartz wool

to improve heat transfer characteristics and provide increased surface area to promote condensation. The current system has gradually evolved as successive problem sources were identified and corrected. Sulfur deposition outside of the condenser has not been eliminated but it has been reduced to a manageable level.

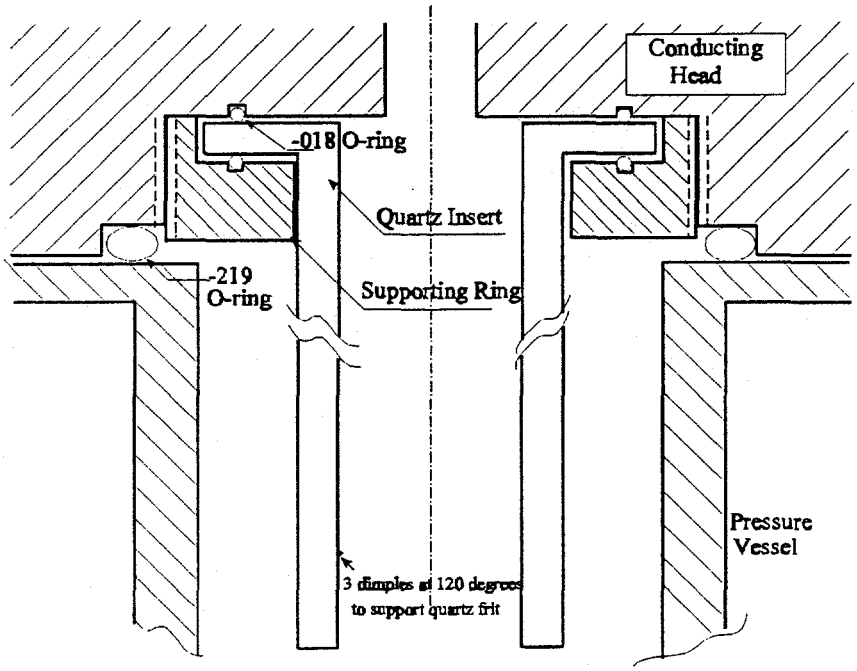


Figure 20. The Quartz Reactor Insert

## Sorbent Properties

From 3 to 6 g of high purity $CeO_2$ from Rhone-Poulenc was used in all tests. Because of the extremely small particle size of the as-received material, pressure drop across the packed bed was approximately 3 atm which placed severe restraints on operating pressure in early tests. With any significant increase in pressure drop, the bed inlet pressure exceeded the $SO_2$ vapor pressure, thereby preventing $SO_2$ flow. This problem was solved by dry pressing the $CeO_2$ powder at 25,000 psi to form tablets, which were subsequently crushed and sieved. Particle size ranges between 150 and 300$\mu$ and between 75 and 150$\mu$ were used in later tests in which the bed pressure drop was only about 5 psi. Severe sintering was also encountered in early tests in which pure $CeO_2$ was used. At the conclusion of the test the sorbent was removed from the reactor as a single, highly porous cylinder. Shrinkage accompanied the sintering and provided an open path around the circumference of the reactor which allowed gas to bypass the sorbent. The sintering problem was solved by physically mixing $CeO_2$ with inert $Al_2O_3$ having a particle size range from 80 to 200$\mu$ to form the packed bed. The mixtures of $Al_2O_3$ and $CeO_2$ formed from the crushed tablets emerged from the reactor as free-flowing powders even after multicycle sulfidation-regeneration tests. Both 1-to-1 and 2-to-1 (by weight) mixtures of $CeO_2$-to-$Al_2O_3$ have been used without problems associated with sintering.

## $CeO_2$ Sulfidation

Although the primary objective of the exploratory tests was to determine the feasibility of producing elemental sulfur directly during the regeneration of $Ce_2O_2S$ using $SO_2$, it was necessary to begin by sulfiding $CeO_2$ since $Ce_2O_2S$ could not be obtained commercially. Each regeneration test was preceded by sulfidation. The reaction parameters and range of reaction conditions studied is summarized in Table 3. The sulfidation gas composition was constant in all tests while pressure was always about 5 atm. In the early runs preceding the $CeO_2$ tableting step previously described, high bed pressure drop resulted in sulfidation pressures slightly above 5 atm. Temperature, gas flow rate, mass of $CeO_2$, and the $CeO_2$-to-$Al_2O_3$ ratio were varied in the preliminary test series.

Sulfidation results from an early "good" test are shown in Figure 21 in the form of a $H_2S$ breakthrough curve. After 20 minutes, the $H_2S$ concentration in the product gas increased to the 0.03% to 0.08% range and remained at that plateau level until 75 minutes. Active breakthrough then began, and an additional 25 minutes were required for the $H_2S$ concentration to increase from 0.1% to 0.9%. A steady-state $H_2S$ concentration of 0.99% was reached after 145 minutes elapsed time. Results of a non-reacting tracer test at the same conditions are also shown in Figure 21. The shaded area between the two curves is proportional to the quantity of $H_2S$ removed by reaction with $CeO_2$. Numerical integration showed that the area corresponded to 102% of the stoichiometric sulfur associated with complete conversion of $CeO_2$ to $Ce_2O_2S$.

The $CeO_2$ tableting procedure was used for the first time in run Ce-09s01. The mass of $CeO_2$ was the same in both Ce-08s01 and Ce-09s01 but less $Al_2O_3$ was used in Ce-09s01 in order to maintain the total bed volume approximately constant. Other reaction conditions were the same in the two runs. The similarity of the $H_2S$ breakthrough curves shown in Figures 21 and 22 in terms of the prebreakthrough plateau, the times corresponding to the beginning of breakthrough, and the slopes of the active portion of the breakthrough curves shows that the larger $CeO_2$ particle size and the different $CeO_2$-to-$Al_2O_3$ ratio had little effect other than to reduce bed pressure drop. All tests subsequent to Ce-09 used the larger $CeO_2$ particles obtained from the crushed tablets.

Table 3. Reaction Parameters in Preliminary $CeO_2$ Sulfidation Studies

| Parameter | Range of Conditions |
|---|---|
| Temperature, °C | 350 to 850 |
| Pressure, atm | 5.0 to 5.4 |
| Gas Composition | 1% $H_2S$ |
| | 10% $H_2$ |
| | balance $N_2$ |
| Gas Flow Rate, sccm | 200 to 400 |
| Mass of $CeO_2$, g | 3.0 to 6.0 |
| $CeO_2$ to $Al_2O_3$ Ratio | 0.5 to 2.0 |

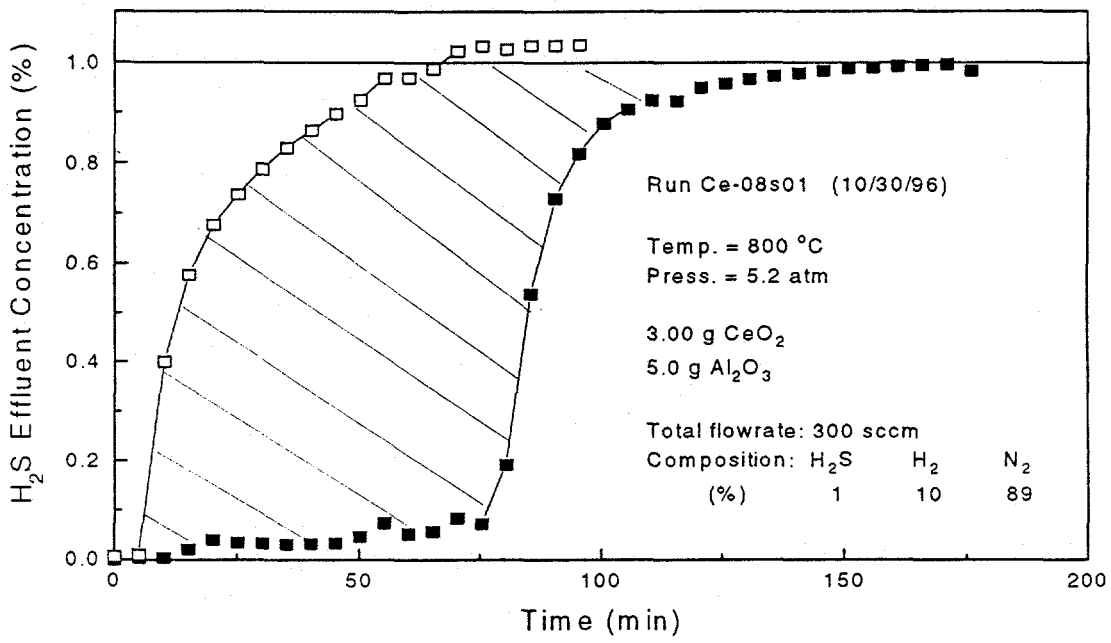


Figure 21. Fixed-Bed Reactor Response: $H_2S$ Breakthrough, Run Ce-08s01

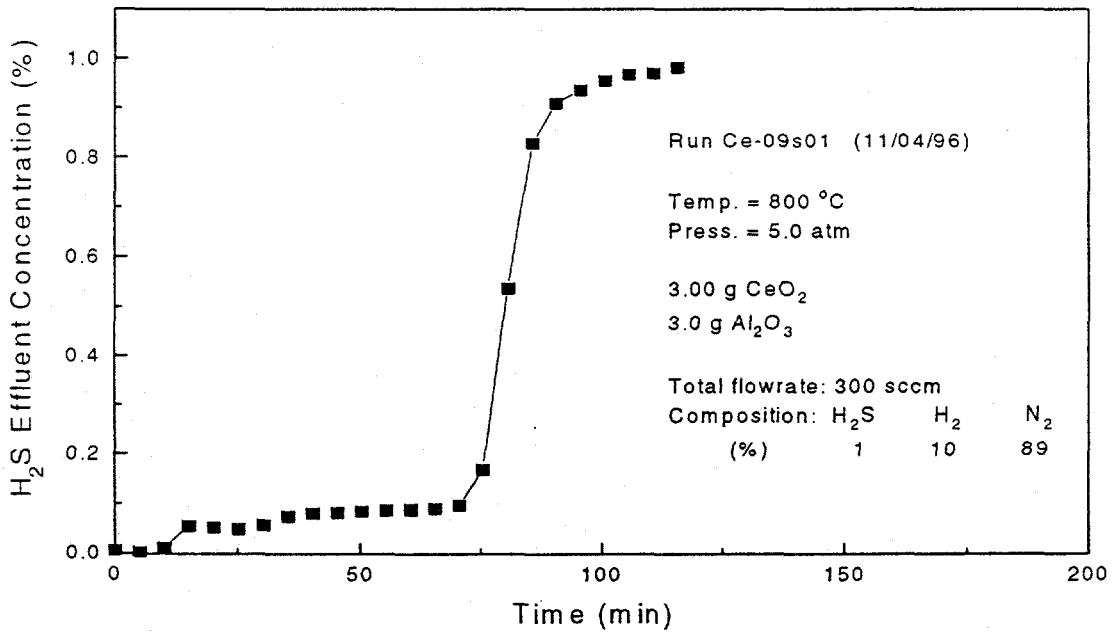


Figure 22. Fixed-Bed Reactor Response: $H_2S$ Breakthrough, Run Ce-09s01

Most sulfidation tests were carried out at 800°C, and the effect of temperature over the range of 700°C to 850°C is quite small as shown in Figure 23. Active breakthrough began after about 60 minutes at the lower temperatures of 700 and 750°C, and after 70 minutes at 800 and 850°C. The slopes of the active portions of the breakthrough curves were approximately equal at 750, 800 and 850°C, but the slope at 700°C was considerably smaller, indicating a decrease in the global reaction rate at the lowest temperature. The postbreakthrough steady-state $H_2S$ concentrations varied from a low of 0.83% at 850°C to a high of 1.08% at 750°C. All steady-state concentrations except the 0.83% at 850°C were within acceptable limits associated with mass flow controller and analytical system errors. The 850°C test was repeated with effectively identical results, so that the reduced postbreakthrough concentration appears to be real. One possible explanation is the increasing importance of the $H_2S$ reaction with the stainless steel pressure vessel at the highest temperature. Substitution of the quartz insert for the stainless steel insert minimized, but did not eliminate, contact between hot steel surface and product gas.

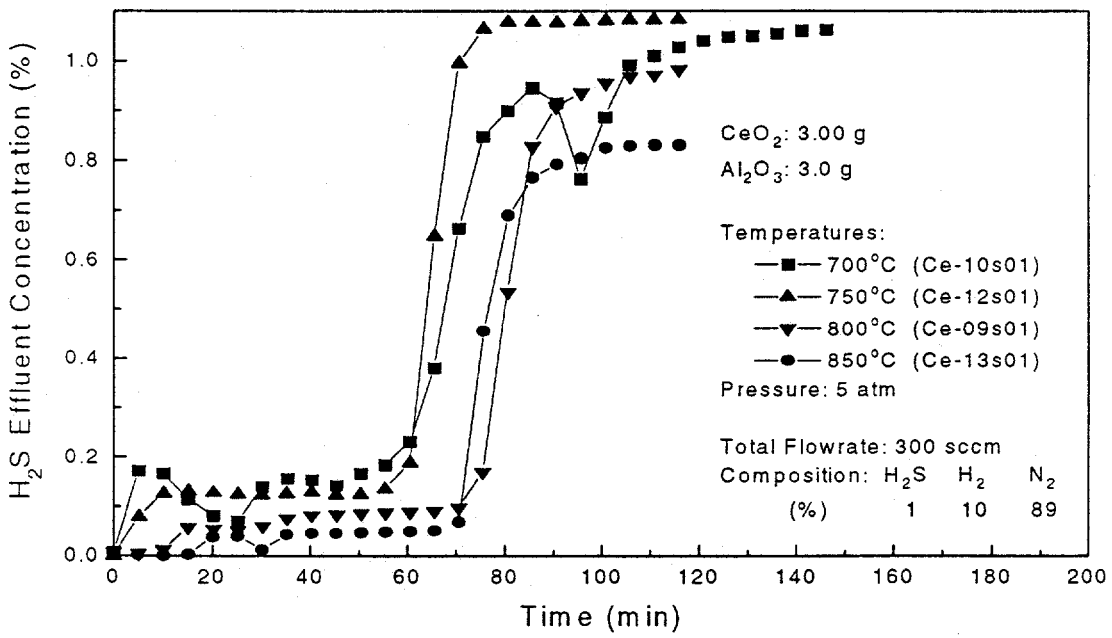


Figure 23. The Effect of Sulfidation Temperature

The prebreakthrough $H_2S$ concentration plateau is also evident in each of the tests shown in Figure 23. The presence of the plateau was not initially a source of concern since primary interest was aimed at the production of elemental sulfur during regeneration. We now believe that the $H_2S$ plateau is caused by reaction between $H_2$ in the sulfidation gas and elemental sulfur deposited in cooler sections of the reactor and downstream tubing during earlier regeneration tests. Evidence in support of this explanation is presented in Figure 24. Following a regeneration test, the reactor and downstream tubing were heated to 800°C and 350°C, respectively. 150 sccm of 10% $H_2$, balance $N_2$ was fed to the reactor, and quite large concentrations of $H_2S$ were formed. An initial surge of about 0.5% $H_2S$ was followed by a gradual decrease to a relatively constant level of 0.2%. After 160

minutes the temperature of the downstream tubing was reduced to 25°C and the gas flow rate was increased to 400 sccm. The $H_2S$ concentration quickly decreased to about 0.01%.

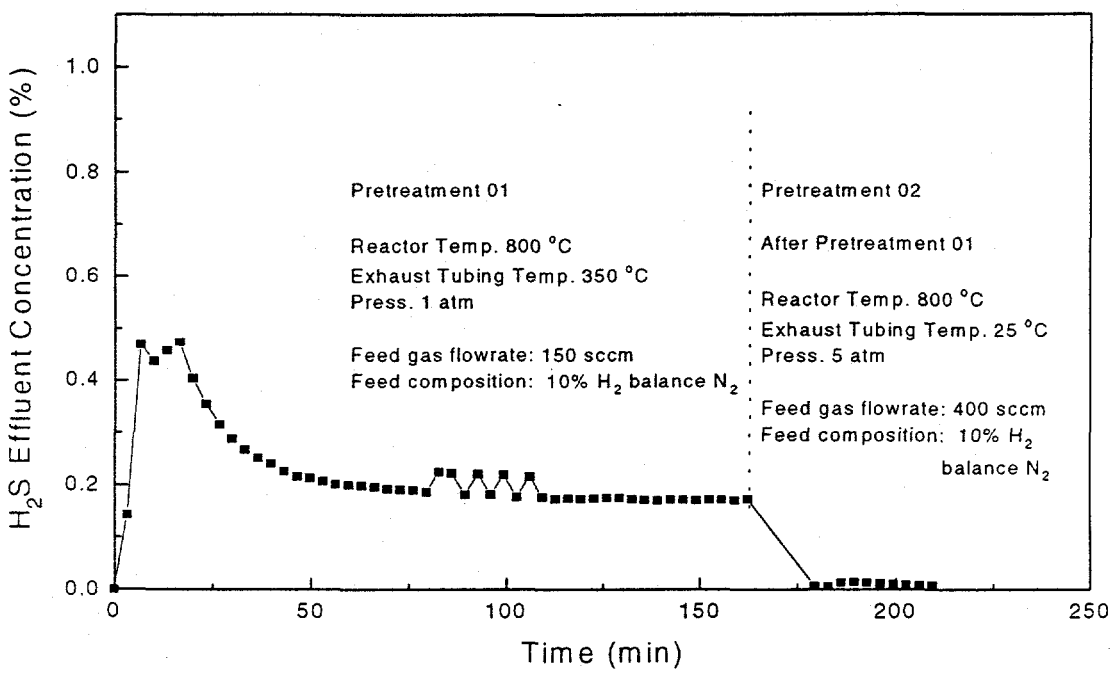


Figure 24. Reactor Cleaning Test: $H_2S$ Formed by the Reaction of $H_2$ and Elemental Sulfur

The $H_2S$ breakthrough curve from run Ce-16s03, the first sulfidation test following the cleaning procedure, is shown in Figure 25. The reduction in $H_2S$ concentration during early portions of the run is obvious. The 0.01% $H_2S$ during the first 20 minutes corresponds to 99% $H_2S$ removal, and the removal remained above 95% for the first 80 minutes of the test. Other characteristics of the breakthrough curve, including the time corresponding to the beginning of active breakthrough and the slope of the active portion of the breakthrough curve, are similar to results from other sulfidation tests at the same conditions.

Additional cleaning studies (not shown) were conducted in which the reactor at 800°C and downstream tubing at 350°C were exposed to flowing air. Appreciable $SO_2$ was found in the product gas meaning that the $H_2$ cleaning was successful in removing most, but not all, of the sulfur contamination. This aspect has not been fully pursued since $H_2S$ is analyzed using the thermal conductivity detector (TCD) whose $H_2S$ sensitivity limit is about 100 ppmv (0.01%). Thus, the measured $H_2S$ concentrations during the first 20 minutes of run Ce-16s03 are near the detection limit. More complete cleaning to further reduce the early $H_2S$ concentration is of limited value until the analytical capability for $H_2S$ is upgraded.

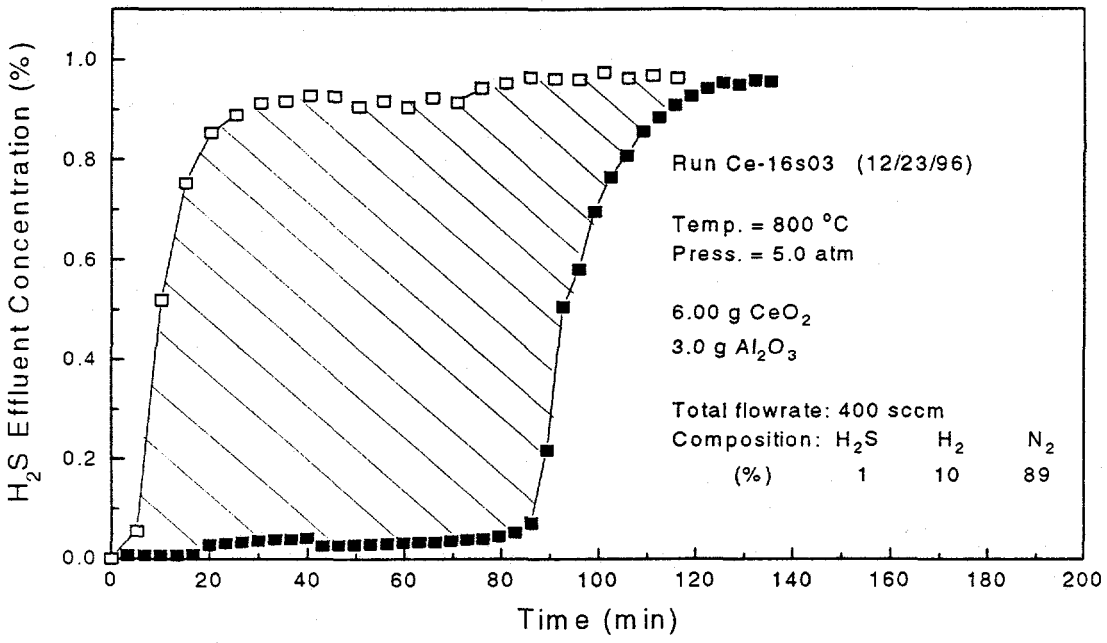


Figure 25. Fixed-Bed Reactor Response: $H_2S$ Breakthrough Curve, Run Ce-16s03

### $Ce_2O_2S$ Regeneration

All regeneration tests were preceded by sulfidation. In addition, all regeneration tests described in the following paragraphs were carried out after the $CeO_2$ tableting procedure was adopted. For the cerium sorbent process to be economical, it is necessary that the elemental sulfur concentration in the regeneration product gas be reasonably large in order that the heat duty of the sulfur condenser and the quantity of recycle $SO_2$ be maintained at reasonable levels.

Reaction parameters and the range of regeneration conditions studied are summarized in Table 4. In the first regeneration test, the initial temperature tested was 350°C, and no reaction was observed. The temperature was then increased gradually and the reaction was found to be rapid at 600°C. All subsequent tests were conducted at 600°C. Most regeneration tests were conducted at 1.0 atmosphere to maximize the difference between the vapor pressure of $SO_2$ and the reactor operating pressure. Regeneration testing began using 1% $SO_2$ in $N_2$ and the $SO_2$ content in later tests was gradually increased to a maximum of 12% as we became comfortable with the behavior of the system. Early regeneration tests used a total flow rate of 300 sccm. However, as the $SO_2$ content increased, the duration of the run and the amount of data collected during the run decreased. Consequently, when the $SO_2$ content was increased to 12%, the flow rate was reduced to 200 sccm which, when coupled with changes in the chromatograph sampling frequency, provided sufficient data to establish the characteristics of the $SO_2$ breakthrough curve.

Table 4. Reaction Parameters in Preliminary $Ce_2O_2S$ Regeneration Tests

| Parameter | Range of Conditions |
|---|---|
| Temperature, °C | 350 to 600 |
| Pressure, atm | 1.0 to 2.7 |
| Gas Composition | 1 to 12% |
| | balance $N_2$ |
| Gas Flow Rate, sccm | 200 to 300 |
| Mass of $CeO_2$, g | 3.0 to 6.0 |
| $CeO_2$ to $Al_2O_3$ Ratio | 1 to 2 |

The $SO_2$ breakthrough curve from an early regeneration test at 2.5 atm using 1% $SO_2$ is shown in Figure 26 along with the results of a non-reacting tracer test at the same conditions. The $SO_2$ concentration was effectively zero for the first 45 minutes while active breakthrough occurred in the 45 to 90 minute time span. A temporary upset in the 70 to 90 minute time period was responsible for the unusual shape of the breakthrough curve during that time. After about 100 minutes, the $SO_2$ concentrations from both the reaction and tracer tests reached steady-state values of 1.04%. According to reaction (11), the elemental sulfur concentration (considered as $S_2$) in the regeneration product is equal to the difference between the $SO_2$ concentrations of the feed and product gases. Thus, the elemental sulfur concentration in the product approached 1% for the major portion of the run. The area between the $SO_2$ breakthrough and tracer curves is proportional to the quantity of elemental sulfur liberated during the reaction. Numerical integration of this area corresponded to 104% of the stoichiometric amount of sulfur based on the initial solid being pure $Ce_2O_2S$. This value is in good agreement with the sulfur material balance during the preceding sulfidation cycle (Ce-09s01) which corresponded to sulfur removal of 110% of stoichiometric based on the initial solid being pure $CeO_2$. The sulfur material balance closures in both the sulfidation and regeneration phases of this test are typical. In most of the exploratory runs the sulfur material balance closure was within ±10% of stoichiometric.

$SO_2$ breakthrough curves for a number of regeneration tests using increasing $SO_2$ concentrations are shown in Figure 27. The concentration axis is normalized, i.e., the ratio of the product and feed concentrations, so that the results from all tests should approach a value of 1.0, which is indeed the case. The beginning of active breakthrough decreased from about 60 minutes to 30 minutes to 15 minutes to between 5 and 10 minutes as the $SO_2$ content increased from 1% to 2% to 4% and finally to 8%. Note that the 2%, 4%, and 8% tests were all part of run Ce-15, and represent the results of three separate sulfidation and regeneration cycles. Multicycle test results are covered in the following section. Also the four tests represent a range of regeneration pressures from 1 to 2.5 atm.

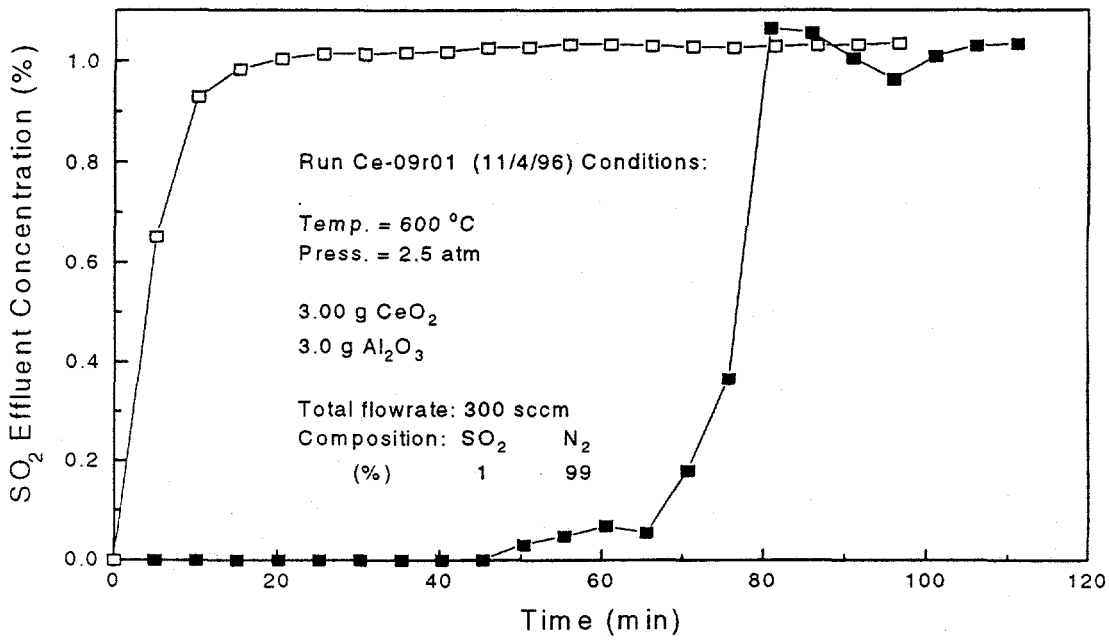


Figure 26. Fixed-Bed Reactor Response: $SO_2$ Breakthrough Curve, Run Ce-09r01

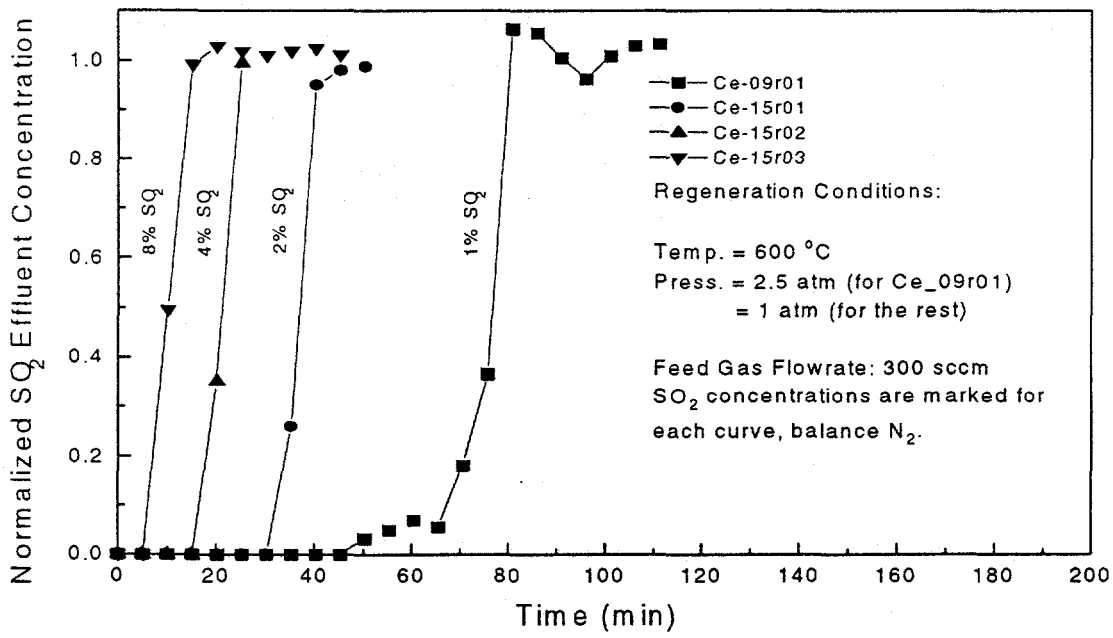


Figure 27. $SO_2$ Breakthrough Curves as a Function of $SO_2$ Content of the Feed Gas

With the exception of the $SO_2$ plateau in the 45 to 60 minute period of the test using 1% $SO_2$, the appearance of all of the breakthrough curves is similar. In particular, the slopes of the breakthrough curves using 2%, 4%, and 8% $SO_2$ are similar. However, as the concentration increased the duration of the tests decreased and fewer product gas samples were available to characterize the breakthrough curve. For example, regeneration using 8% $SO_2$ was effectively complete by the fourth sample about 16 minutes after the start of the test. The relative sparcity of the data may be responsible for the lack of the $SO_2$ concentration plateau at the higher $SO_2$ concentrations.

Because of the shorter duration and limited number of product gas concentration data points, it was obvious that changes in the operating conditions were required before further increases in $SO_2$ concentration could be made. The conclusion of the exploratory test phase called for a ten cycle run at still larger $SO_2$ concentration to provide preliminary information on the durability of the $CeO_2$ sorbent. Three significant changes were made prior to the multicycle test. The chromatograph operating conditions were altered to reduce the product gas sampling interval from 5.0 to 3.3 minutes. The regeneration gas flow rate was reduced from 300 to 200 sccm in order to maintain a constant $SO_2$ flow rate of 24 sccm while increasing the $SO_2$ content from 8% to 12%. Finally, the amount of the $CeO_2$ charge was doubled from 3.0 to 6.0 g. The amount of $Al_2O_3$ was constant at 3.0 g in each test.

## Multicycle Test Results

The key to any high temperature desulfurization process is sorbent durability. Therefore a ten-cycle run, Ce-16, was conducted to provide preliminary information on the durability of the $CeO_2$ sorbent. Planned reaction conditions for the sulfidation and regeneration cycles are presented in Table 5. Unfortunately, an error in the total gas flow rate was made in the first sulfidation cycle, Ce-16s01, and results from this test are not included in the following discussion.

Table 5. Sulfidation and Regeneration Conditions for Ten-Cycle Test Ce-16

Reactor Charge

6.0g $CeO_2$
3.0g $Al_2O_3$

| Sulfidation | | Regeneration | |
|---|---|---|---|
| Temperature, °C | 800 | Temperature, °C | 600 |
| Pressure, atm | 5 | Pressure, atm | 1 |
| Gas Composition, % | | Gas Composition, % | |
| $H_2S$ | 1 | $SO_2$ | 12 |
| $H_2$ | 10 | $N_2$ | 88 |
| $N_2$ | 89 | | |
| Flow Rate, sccm | 400 | Flow Rate, sccm | 200 |

$H_2S$ breakthrough curves for nine cycles, Ce-16s02 through Ce-16s10, are shown in Figures 28 and 29. Figure 28 is the traditional figure showing the entire breakthrough curve while in Figure 29 the concentration scale has been expanded to emphasize $H_2S$ concentrations during the prebreakthrough period. Note that the breakthrough curve for Ce-16s08 is different from the other curves. The $H_2S$ mass flow controller malfunctioned after 175 minutes causing the $H_2S$ flow rate to decrease and producing the decreasing $H_2S$ concentrations; this malfunction may have begun earlier and been responsible for the earlier differences in the Ce-16s08 breakthrough behavior as well.

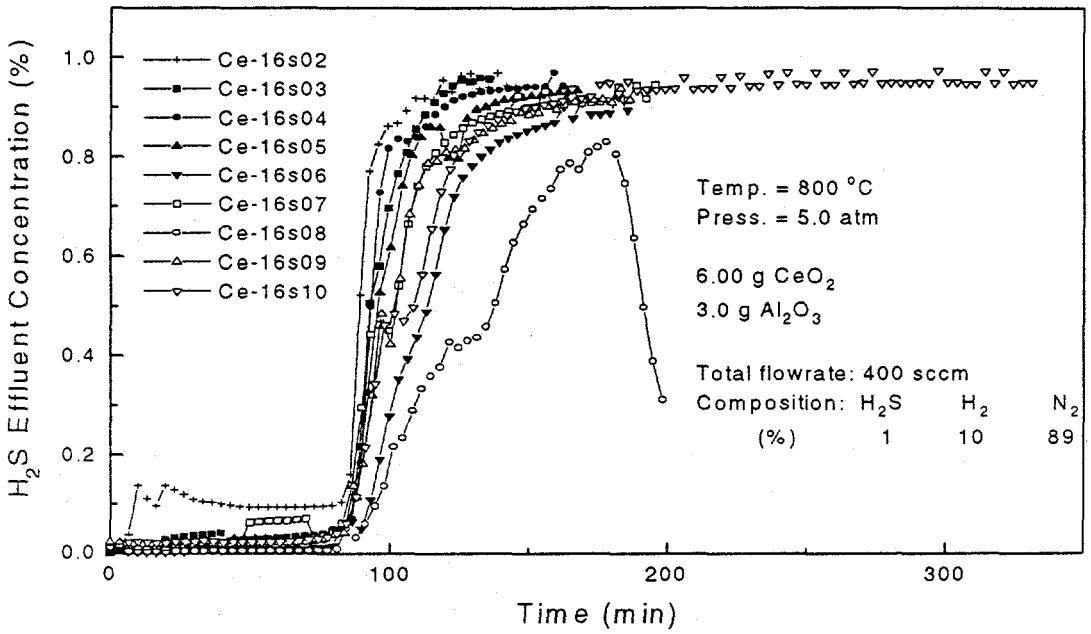


Figure 28. Fixed-Bed Reactor Response: $H_2S$ Breakthrough Curves for Nine Sulfidation Cycles of Run Ce-16 Showing the Entire Breakthrough Curves

These figures show a wide variation in prebreakthrough behavior. The prebreakthrough concentration in Ce-16s02 is about 0.1% $H_2S$ which corresponds to only 90% $H_2S$ removal. However, in all other cycles the initial concentrations were equal to or less than 0.025% $H_2S$ (250 ppmv), and, with the exception of the unexplained upset in Ce-16s07 during the 50 to 70 minute period, the $H_2S$ concentrations were less than 0.05% (500 ppmv, 95% removal) for about 80 minutes in each cycle. Of particular interest, the concentrations in Ce-16s06 and Ce-16s08 were below 150 ppmv for the first 80 minutes. $H_2S$ breakthrough time, which is taken to correspond to 0.05% $H_2S$, was approximately constant as shown in Figure 30. The breakthrough times ranged from 79.5 minutes in Ce-16s04 to 84.3 minutes in Ce-16s05 with no visible decrease as the cycle number increased. Results from Ce-16s01 and Ce-16s02 are omitted from the figure and the upset in Ce-16s07 was ignored in determining the breakthrough time.

The importance of sulfur contamination from preceding regeneration runs was discovered between cycles Ce-16s02 and Ce-16s03. Various cleaning procedures were used beginning with Ce-16s03 and all subsequent prebreakthrough concentrations were significantly lower. Most of the sulfur

contaminant was removed by flowing sulfur-free reducing gas through the reactor at 850°C and tubing located between the reactor and condenser heated to 350°C. The prebreakthrough concentrations in Ce-16s03 through Ce-16s10 in Figure 29 followed cleaning in the reducing gas. Reduction, however, was not sufficient to remove all sulfur compounds since significant $SO_2$ concentrations were formed when air flowed through the reactor and tubing at high temperature.

All ten regeneration cycles used the reaction conditions shown in Table 5, and $SO_2$ breakthrough curves for all cycles are shown in Figure 31. With the exception of two individual samples -- the first at 17 minutes in Ce-16r03 and the second at 10 minutes in Ce-16r10 -- the results

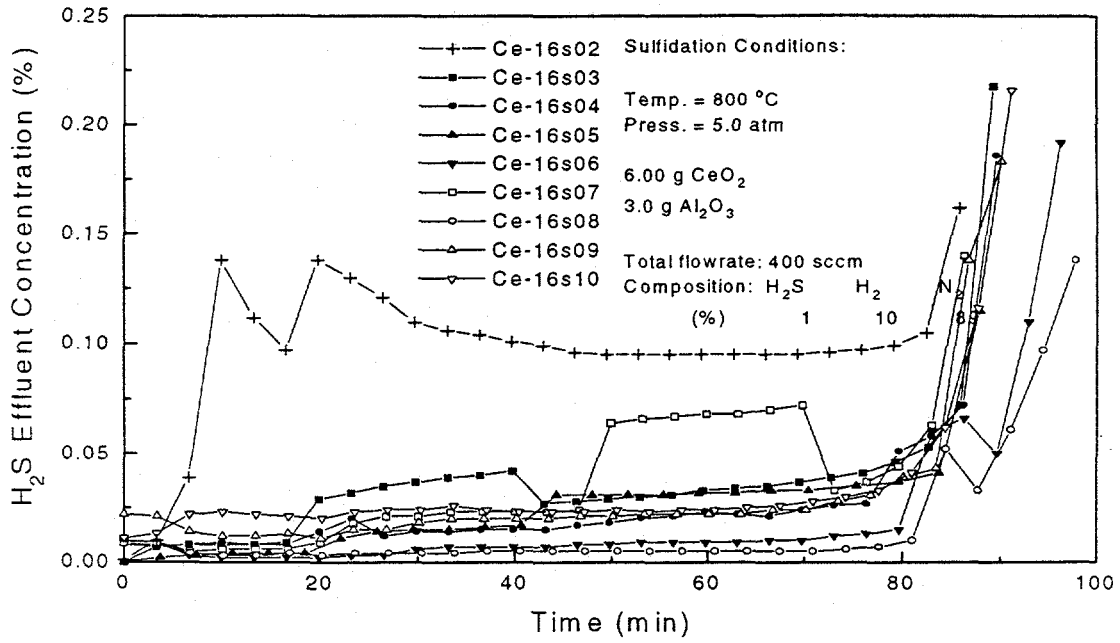


Figure 29. Fixed-Bed Reactor Response: $H_2S$ Concentration During the Prebreakthrough Periods of Run Ce-16

were effectively identical. The first measurable concentration of $SO_2$, about 1%, was detected after 10 minutes, and by 23 minutes regeneration was effectively complete. The steady-state $SO_2$ content of the product gas ranged from 11.8% to 12.2%.

Sulfur material balance results, expressed as percent of stoichiometric sulfur removed during sulfidation and liberated during regeneration, are presented in Figure 32. Sulfur removed during sulfidation ranged from a minimum of 75.0% in Ce-16s02 to a maximum of 96.8% in Ce-16s10. No sulfidation results are presented for Ce-16s01 because of the flow rate error and for Ce-16s08 because of the $H_2S$ mass flow controller malfunction. The low value in Ce-16s02 may be associated with the high prebreakthrough $H_2S$ concentration (see Figures 28 and 29) caused by residual sulfur from the previous regeneration cycle. For the eight sulfidation cycles, $H_2S$ removal averaged 87.2% of stoichiometric (88.9% of stoichiometric if the low value associated with Ce-16s02 is not considered).

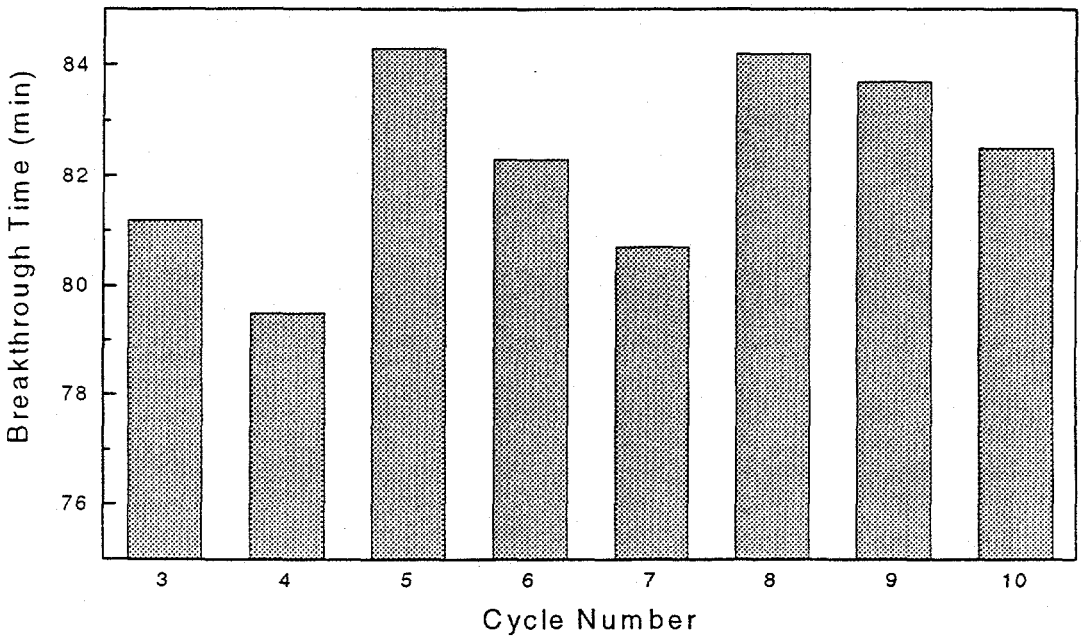


Figure 30. Breakthrough Times Corresponding to 0.05% $H_2S$ in the Product Gas of Run Ce-16

Sulfur material balance during regeneration ranged from 86.1% stoichiometric in Ce-16r03 to 96.2% in Ce-16r10 with a ten-cycle average of 91.8% of stoichiometric. Ideally, the sulfidation and regeneration results from a single cycle should be identical. That is, the quantity of sulfur removed during sulfidation should be equal to the quantity liberated during regeneration. Differences are caused by errors in flow rates (mass flow controllers), product gas analysis and numerical integration of the breakthrough data. The maximum difference occurred in cycle 02 where sulfur removal was 75.0% of stoichiometric and sulfur liberation was 90.4% of stoichiometric. However, the agreement is quite good based on the average results of the entire test; as previously stated, the average sulfur removal from the eight sulfidation tests was 87.2% of stoichiometric (88.9% ignoring cycle 02) while the ten-cycle regeneration average was 91.8% of stoichiometric.

The overall results from this first extended test are considered to be quite favorable. The constancy of the slopes of the sulfidation and regeneration curves during active breakthrough, the small variation in breakthrough times, and the reasonable agreement in sulfur material balance during sulfidation and regeneration all suggest that little, if any, sorbent deterioration occurred.

Test Ce-16 ended the exploratory phase of the experimental program. Favorable experimental results coupled with reasonable economic projections from the process analysis effort (not discussed in this report) lead to the selection of the $CeO_2$ system for more detailed experimental testing. A brief description of plans for the remaining portion of the study is included in the following section.

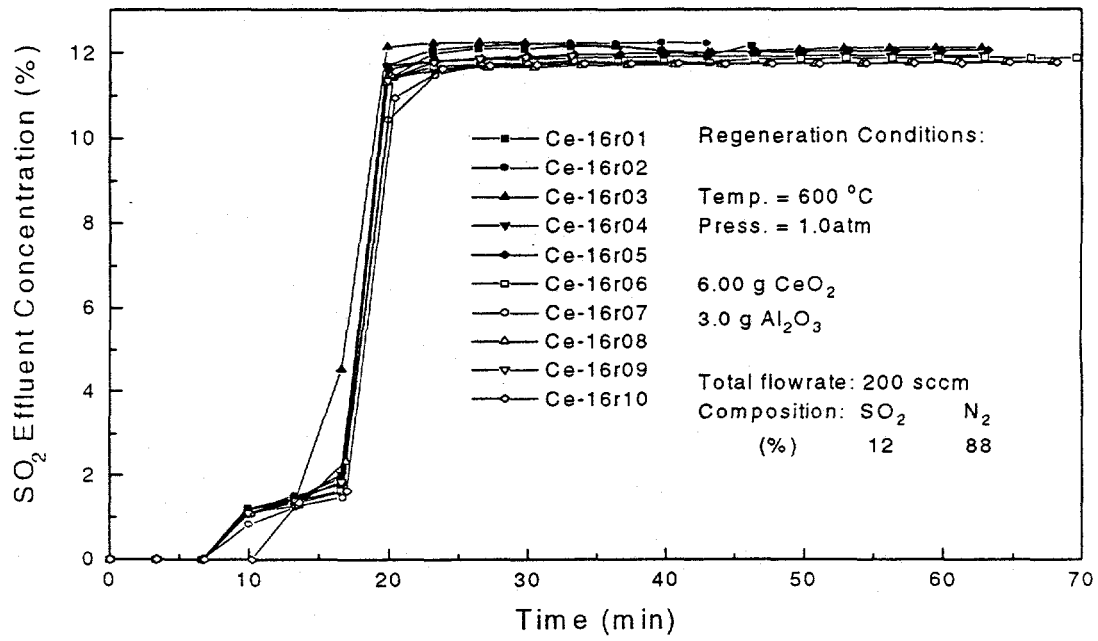


Figure 31. Fixed-Bed Reactor Response: $SO_2$ Breakthrough Curves for the Ten Regeneration Cycles of Run Ce-16

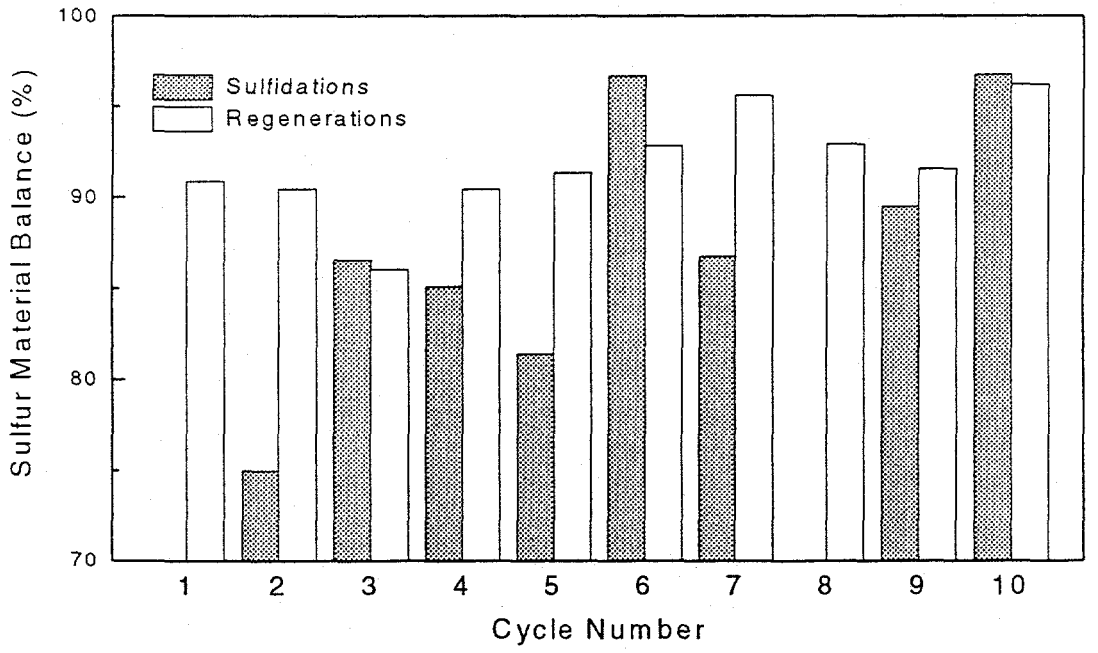


Figure 32. Sulfur Material Balance Closure During the Ten Sulfidation and Regeneration Cycles of Run-16

## SUMMARY AND FUTURE EXPERIMENTAL WORK

The exploratory experimental phase of this project examined the regeneration of FeS under "partial oxidation" conditions and the sulfidation of $CeO_2$ with $H_2S$ and regeneration of $Ce_2O_2S$ with $SO_2$. The objective of both regeneration studies was the direct production of elemental sulfur

While large fractions of the sulfur in FeS can be successfully liberated in elemental form, the reaction must operate under $O_2$-starved conditions and with a large excess of steam. As a result, the elemental sulfur concentration of the regeneration product gas is judged to be too low for commercial application. Energy costs associated with providing the large amounts of steam, and subsequent cooling costs to recover elemental sulfur would be excessive.

In contrast, the regeneration of $Ce_2O_2S$ with $SO_2$ proceeds rapidly at 600°C with stoichiometric production of elemental sulfur. As much as 12% elemental sulfur has been produced in the regeneration product gas during this exploratory effort, and there appears to be no fundamental reason why significantly higher concentrations cannot be produced. Essentially pure elemental sulfur can be separated by condensation with excess $SO_2$ recycled to the regeneration reactor. No evidence of $CeO_2$ sorbent deterioration was seen in a ten-cycle test. While numerous experimental problems caused by elemental sulfur condensing and plugging the laboratory-scale experimental apparatus were experienced, such problems should be relatively easy to control in a commercial process.

The potential problems with a $CeO_2$ process are concentrated in the desulfurization phase. The thermodynamics of the $CeO_2$-$H_2S$ reaction are not sufficient under most circumstance to reduce the $H_2S$ concentration to levels needed for IGCC operation. For this reason, a two-stage desulfurization process using $CeO_2$ for bulk $H_2S$ removal followed by a polishing step using zinc sorbent has been proposed. Elemental sulfur would be produced during the regeneration of $Ce_2O_2S$ while $SO_2$ formed during ZnS regeneration would be recycled to the gasifier and ultimately captured as elemental sulfur.

The required temperature for sulfidation of $CeO_2$ is approximately 800°C, considerably above the maximum temperature at which zinc sorbents are applicable. Although reduction of $CeO_2$ to $CeO_n$ ($n<2$) is known to occur in highly reducing gases at sufficiently high temperature, no volatile products are formed as with Zn(g). Indeed, reduction and subsequent sulfidation of $CeO_n$ offers promise for increased $H_2S$ removal compared to $CeO_2$ and creates the possibility that a single-stage cerium sorbent process might by used in limited conditions. Determining the ultimate desulfurization capability of $CeO_n$ provides a major objective for the remainder of the project.

The gas chromatograph currently used for gas analysis is equipped with a thermal conductivity detector whose sensitivity limit for $H_2S$ is about 100 ppmv. A flame photometric detector will be acquired to enable the $H_2S$ analysis to be extended to low (<10) ppmv levels. Sulfidation product gas analysis at these low $H_2S$ concentrations will also require that the reactor and downstream tubing be free from sulfur contamination from previous regeneration tests. Modifications in the reactor system to insure the required level of cleanliness are being planned.

During the remainder of the study, the effects of reaction parameters such as temperature, pressure, gas flow rate and composition will be examined. $CeO_2$ from three sources will be tested and durability studies will be extended to at least 20 sulfidation-regeneration cycles. Primary emphasis during the sulfidation phase will be devoted to determining if $H_2S$ concentrations of 20 ppmv or less can be achieved, and, if so, over what range of conditions. Because of the importance of system cleanliness in achieving low $H_2S$ concentration, the regeneration phase may be omitted in some of these sulfidation tests.

The objective of the regeneration studies will be increase the maximum elemental sulfur concentration from the current 12% to perhaps 20%. From the process analysis effort accompanying the experimental study, it appears that the optimum elemental sulfur concentration should be about 15%. In addition, we will examine the effect of the reaction parameters to provide guidance for additional larger-scale studies in fluidized-bed reactors.